Amplitude analysis (AA) of $e^+e^- \to \pi^+\pi^-2\pi^0$ and $e^+e^- \to 2\pi^+2\pi^-$ reactions with the CMD-3 detector

Evgeny Kozyrev
BINP, NSU
e.a.kozyrev@inp.nsk.su
01.03.2019

Novosibirsk State University
*THE REAL SCIENCE

1. For the measurement of the **cross section of the $e^+e^- \to 4\pi$** reaction we are required to find out which intermediate states are involved in this process in order to obtain a correct value of detection efficiency.

2. The AA allows to describe experimental data by phenomenological **model**.

3. Actually, the phenomenological approach is far from the **fundamental understanding** of the process of the hadronization of the produced pair of quarks and of four pions production.

Novosibirsk State University
*THE REAL SCIENCE

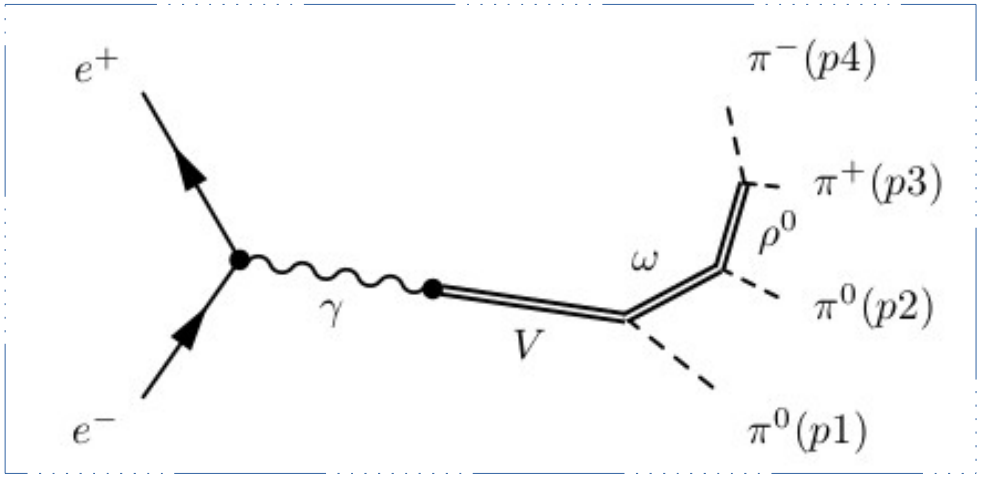
e^+
e^-
γ
V
ω
ρ^0
$\pi^-(p4)$
$\pi^+(p3)$
$\pi^0(p2)$
$\pi^0(p1)$

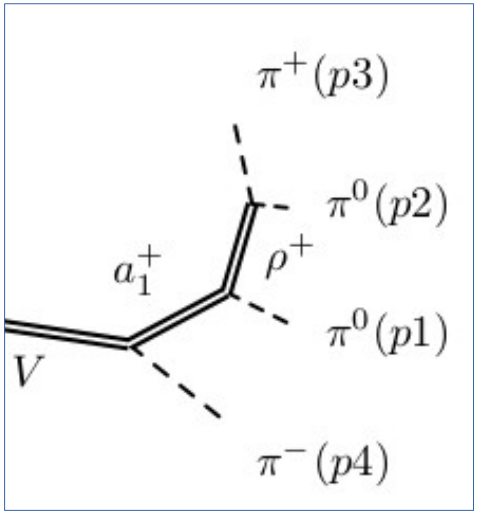
$\pi^+(p3)$
a_1^+
ρ^+
$\pi^0(p2)$
V
$\pi^0(p1)$
$\pi^-(p4)$

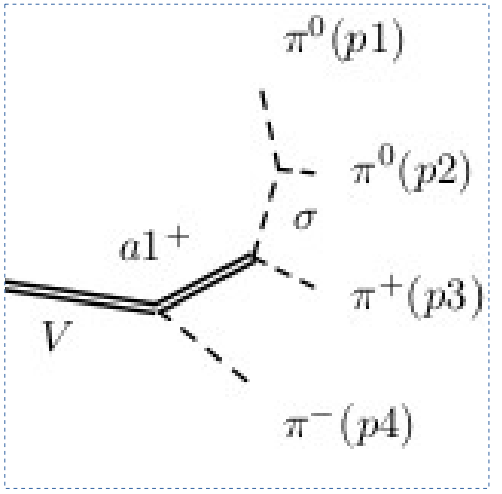
$\pi^0(p1)$
$\pi^0(p2)$
σ
$a1^+$
$\pi^+(p3)$
V
$\pi^-(p4)$

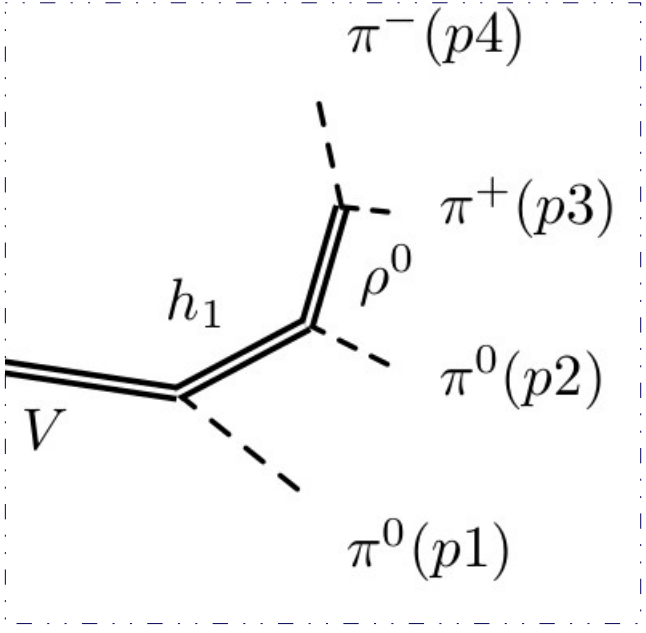
$\pi^-(p4)$
$\pi^+(p3)$
h_1
ρ^0
$\pi^0(p2)$
V
$\pi^0(p1)$

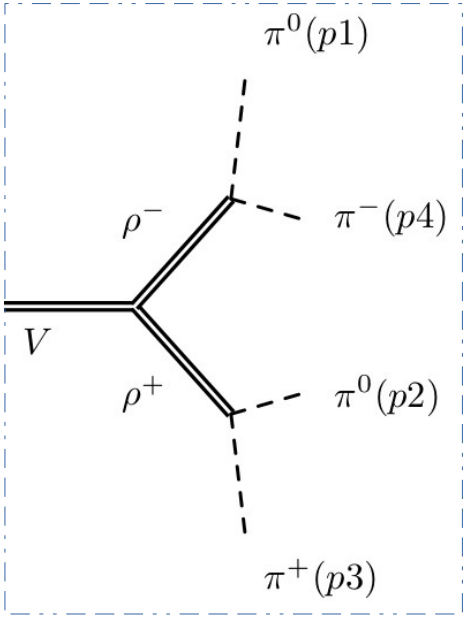
$\pi^0(p1)$
ρ^-
$\pi^-(p4)$
V
ρ^+
$\pi^0(p2)$
$\pi^+(p3)$

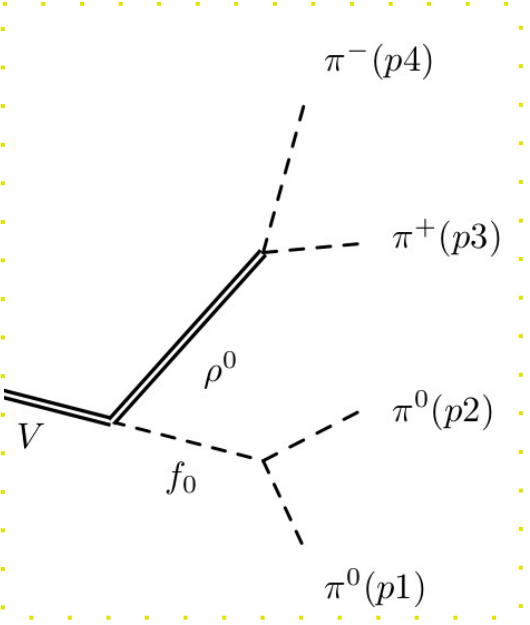
$\pi^-(p4)$
$\pi^+(p3)$
ρ^0
$\pi^0(p2)$
V
f_0
$\pi^0(p1)$

The amplitude analysis at CMD-2 (5.8 pb^{-1})

- The data in the $ee \to \pi^+\pi^-2\pi^0$ (22128 events) with $\sqrt{s}$ = [1.05–1.38] GeV is used
- The dominance of the $\omega\pi$ and $a_1\pi$ is proved

The results of a search for the admixture of other possible states

Model	L_{min}	r_X [%]	U.L. [%]
$\omega\pi^0 + a_1\pi$	1264	–	–
$\omega\pi^0 + a_1\pi + \rho\sigma$	1256	$2.1^{+1.2}_{-0.9}$	4.3
$\omega\pi^0 + a_1\pi + h_1\pi$	1263	$0.1^{+0.2}_{-0.1}$	0.4
$\omega\pi^0 + a_1\pi + a_2\pi$	1263	$0.2^{+0.4}_{-0.2}$	0.8
$\omega\pi^0 + a_1\pi + \pi'\pi$	1250	$9.5^{+3.2}_{-2.8}$	15.
$\omega\pi^0 + a_1\pi + \rho^+\rho^-$	1246	$4.7^{+2.0}_{-1.6}$	7.7

R.R. Akhmetshin et al., Physics Letters B ***466***, 392–402 *(1999)*

- The data in $ee \to \pi^+\pi^-2\pi^0$ and $ee \to 2\pi^+2\pi^-$ (28552) is used for the estimation: $B(a_1\to\sigma\pi)/B(a_1\to\rho\pi) \sim 0.3$
- The measured cross section are systematically shifted from other measurement.

Amplitude analysis of $\tau \to 3\pi\pi^0\nu_\tau$ at CLEO (1999)

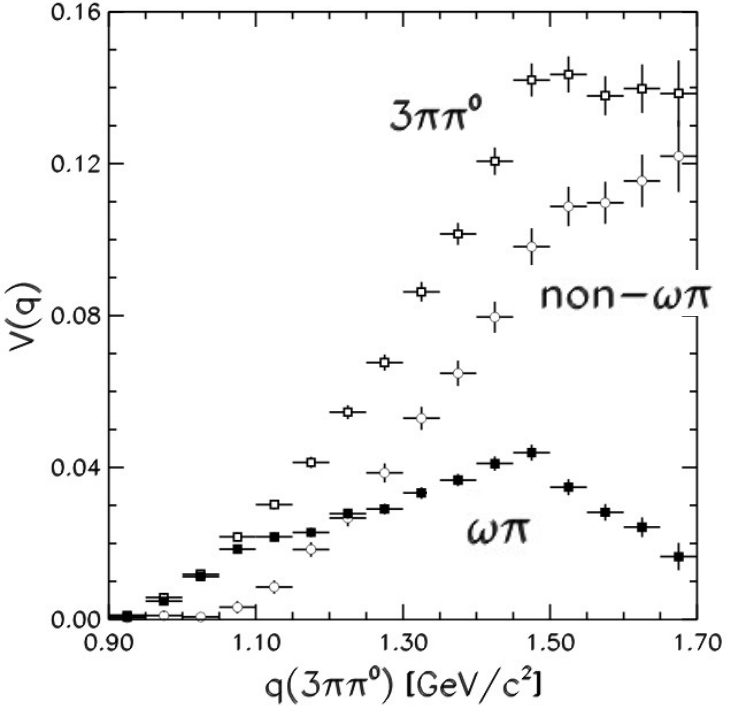

Spectral functions

$$\frac{\Gamma(\tau^- \to \nu_\tau 2\pi^-\pi^+\pi^0)}{\Gamma(\tau^- \to \nu_\tau e^-\overline{\nu}_e)} = \frac{3\cos^2\theta_c}{2\pi\alpha^2 m_\tau^8}\int_0^{m_\tau^2} dQ^2 Q^2 (m_\tau^2 - Q^2)^2 (m_\tau^2 + 2Q^2) \cdot \left[\frac{1}{2}\sigma_{e^+e^-\to 2\pi^-2\pi^+}(Q^2) + \sigma_{e^+e^-\to\pi^+\pi^-2\pi^0}(Q^2)\right]$$

Model	Integrated amplitudes	Goodness-of-fit
Model 2	$R_{\omega\pi} = 0.38 \pm 0.02 \pm 0.02$ $R_{a_1\pi} = 0.43 \pm 0.02 \pm 0.02$	$< 5\%$
Model 3	$R_{\omega\pi} = 0.38 \pm 0.02 \pm 0.01$ $R_{a_1\pi} = 0.49 \pm 0.02 \pm 0.02$ $R_{\sigma\rho} = 0.01 \pm 0.02 \pm 0.01$ $R_{f_0\rho} = 0.01 \pm 0.01 \pm 0.01$	20%

Fit results for various models

- Model with $\omega\pi$ and $a_1\pi$ and $\rho\sigma$, ρf_0 provides the best description of the data.

Physical Review D - Particles, Fields, Gravitation and Cosmology, ***61****, 1-16 (2000).*

There are evidences of ρf_0 and ρf_2 at higher energies with BaBar detector

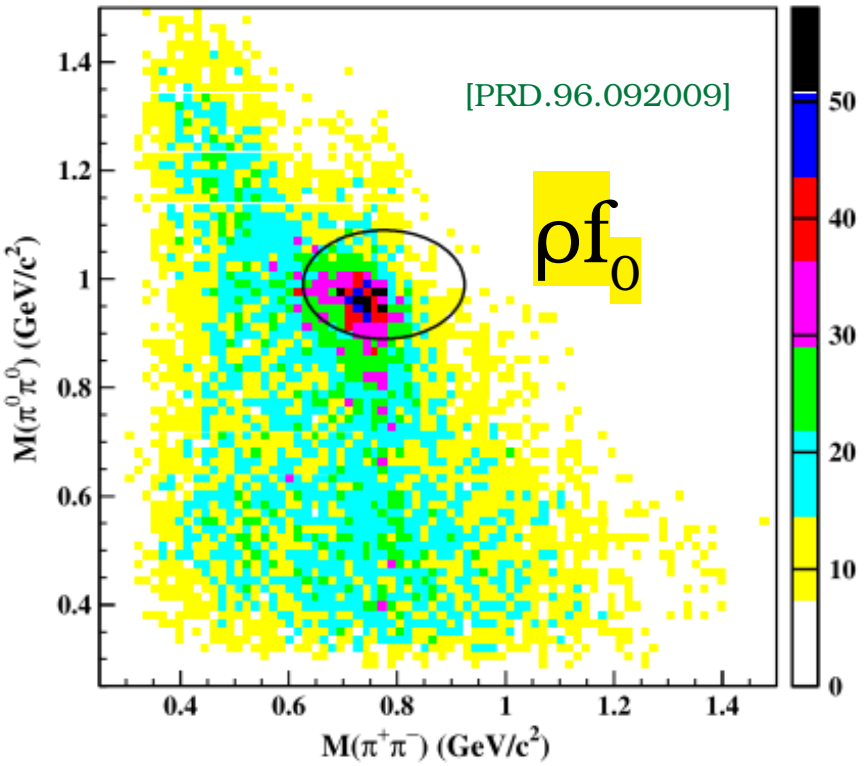

The evidence of ρf_0 in the process e+e- → 2pi0pi-pi+ with BaBar

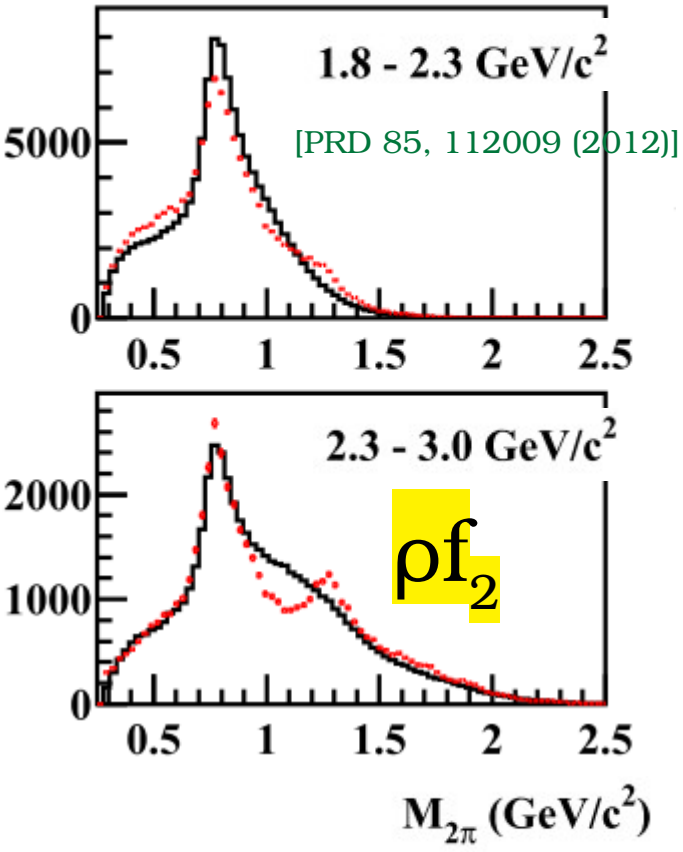

Two pion invariant mass spectra in the process e+e- → 2pi+2pi-

General strategy

Signal selection
($ee \to \pi^+\pi^- 2\pi^0$)

Signal selection
($ee \to 2\pi^+ 2\pi^-$)

Building of the amplitudes formalism

The definition and minimization of likelihood function (L)

Model vs Experiment comparison

Signal selection ($ee \to \pi^+\pi^-2\pi^0$) 64 kevents

- $0.7 < \theta_{\pi,\gamma} < \pi - 0.7$ rad
- Total (E-√s) and P < 150 MeV/(c)
- Two candidates for π^0
- 5C kinematic fit
- The invariant mass spectrum of 3rd and 4th photons is used for the estimation of the contribution of background:

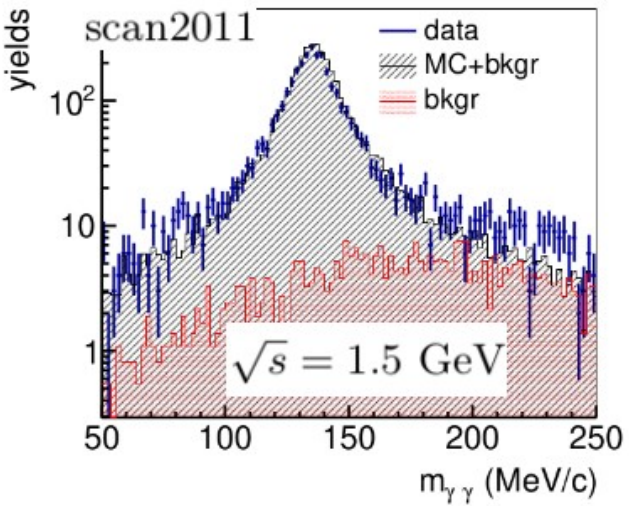

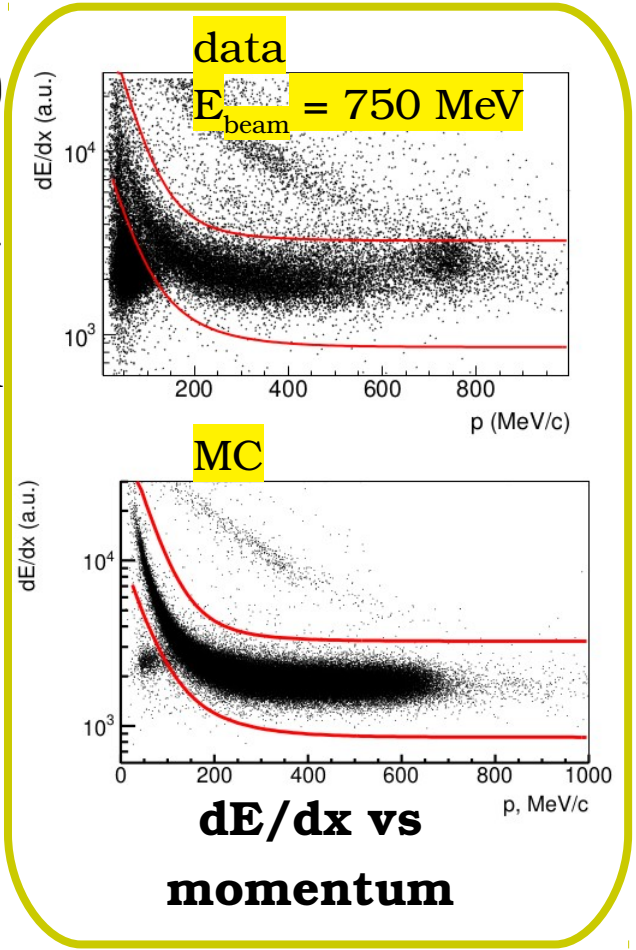

Signal selection ($ee \to 2\pi^+2\pi^-$) 72 kevents

- $0.7 < \theta_{\pi} < \pi - 0.7$ rad
- Total (E-√s) and P < 150 MeV/(c)
- 4C kinematic fit
- The spectrum of total energy of four tracks (E-√s) is used for the estimation of the contribution of background:

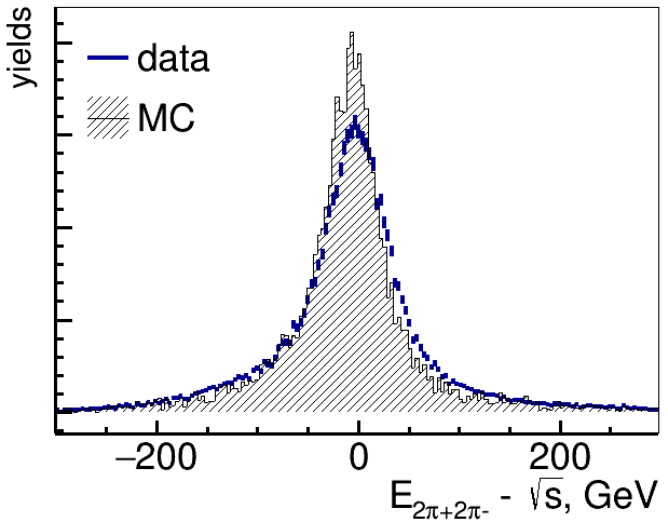

The production of 4π system can proceed via a list of intermediate states:

- $\omega[1^{--}]\ \ \pi^0[0^{-+}]$ (Only $2\pi^{\pm}2\pi^0$)
- $a_1(1200)[1^{+}]\ \ \pi[0^{-}]$
- $\rho[1^{--}]\ \ f_0(980)[0^{++}]$
- $\rho[1^{--}]\ \ \sigma(500)[0^{++}]$
- $\rho[1^{--}]\ \ f_2(1270)[2^{++}]$
- $\rho^{+}[1^{-}]\ \ \rho^{-}[1^{-}]$ (Only $2\pi^{\pm}2\pi^0$)
- $a_2(1320)[2^{++}]\ \ \pi[0^{-}]$
- $h_1(1170)[1^{+-}]\ \ \pi^0[0^{-+}]$ (Only $2\pi^{\pm}2\pi^0$)

To get magnitudes of amplitudes we perform unbinned likelihood amplitude analysis. The relative number of events I at a particular point Ω in phase space can be represented as

$$I(\Omega) = |V_\alpha A_\alpha(\Omega)|^2 \cdot d\Phi(\Omega),$$

where the sum runs over all intermediate states, V_α - the complex production amplitude (the free parameter) and $A_\alpha(\Omega)$ - the amplitude at a particular point in phase space.

The likelihood for model under test is

$$L = -log \prod_{i=signal}^{\boldsymbol{pi^+pi^-2pi^0}} \frac{I(\Omega_i)}{\int \varepsilon I(\Omega) d\Omega} - log \prod_{i=signal}^{\boldsymbol{2pi^+2pi^-}} \frac{I(\Omega_i)}{\int \varepsilon I(\Omega) d\Omega}$$

The limited acceptance and efficiency of the detector is taken into account by summing only over simulated events that pass the reconstruction and analysis cuts.

$$\int \varepsilon I(\Omega) d\Omega = \frac{1}{N_{MC}^{gen}} \sum_{rec}^{phase\ space\ MC} |V_\alpha A_\alpha(\Omega)|^2$$

- An amplitude is normalized to 1: $\int |A_\alpha(\Omega)|^2 d\Omega = 1$;
- The $\omega\pi^0$ amplitude is clearly seen at all energies, so $A_{\omega\pi^0}$ fixes at 1;

- The amplitudes is symmetric (anti-symmetric) with respect to the interchange of the momenta of neutral (charged) mesons according to Bose symmetry and C-parity conservation.
-

$$L(\omega\rho\pi) = g_{\omega\rho\pi} \cdot \epsilon_{\mu\nu\rho\sigma} \cdot \delta^{ab} \cdot \omega_\mu \cdot d_\nu \pi^{\star a} \cdot (d_\rho \rho^{\star b}_\sigma - d_\sigma \rho^{\star b}_\rho),$$

$$L(a_1\rho\pi) = g_{a_1\rho\pi} \cdot \epsilon^{abc} \cdot a^a_{1\mu} \cdot d_\nu \pi^{\star b} \cdot (d_\mu \rho^{\star c}_\nu - d_\nu \rho^{\star c}_\mu),$$

$$L(a_1\sigma\pi) = g_{a_1\sigma\pi} \cdot \delta^{ab} \cdot (d_\mu a^a_{1\nu} - d_\nu a^a_{1\mu}) \cdot d_\mu \phi^\star(\sigma) \cdot d_\nu \phi^{\star b}(\pi),$$

$$L(\rho' \rho f_0) = g_{\rho' \rho f_0} \cdot \delta^{ab} \cdot (d_\mu \rho'^a_\nu - d_\nu \rho'^a_\mu)(d_\mu \rho^{\star b}_\nu - d_\nu \rho^{\star b}_\mu) \cdot \phi^\star_{f0},$$

$$L(\rho' \rho^+ \rho^-) = g_{\rho' \rho^+ \rho^-} \cdot \epsilon^{abc} (d_\mu \rho'^a_\nu - d_\nu \rho'^a_\mu) \cdot (d_\alpha \rho^{\star b}_\nu - d_\nu \rho^{\star b}_\alpha) \cdot (d_\mu \rho^{\star c}_\alpha - d_\alpha \rho^{\star c}_\mu)$$

$$L(\rho' h_1 \pi^\upsilon) = g_{\rho' h_1 \pi^0} \cdot \delta^{ab} (d_\mu \rho'^a_\nu - d_\nu \rho'^a_\mu) \cdot (d_\mu h^{\star b}_{1\nu} - d_\nu h^{\star b}_{1\mu}) \phi^\star_\pi,$$

- Masses and central values of widths of resonances are fixed according to PDG.
- Spectral function obtained from the Dyson equation with simplest π-σ coupling is used as the propagator of σ(500) [*Phys. Rev. C* ***76*** *065204 (2007)*]
- Flatt´ e distribution is used for the propagator of f_0(980).

(ee → pi⁺pi⁻2pi⁰)

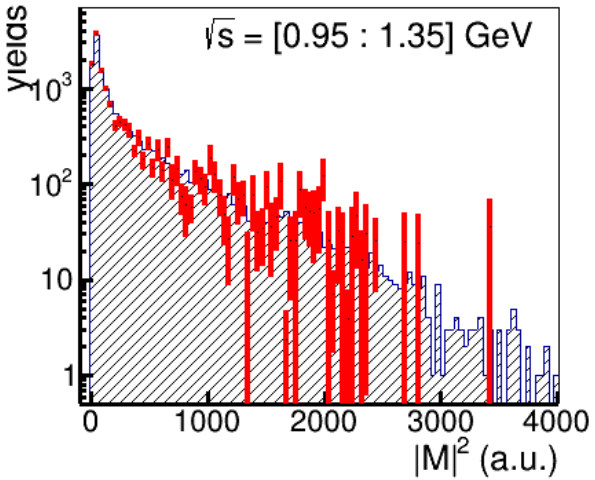
√s = [0.95 : 1.35] GeV
yields
10^3
10^2
10
1
0
1000
2000
3000
4000
$|M|^2$ (a.u.)

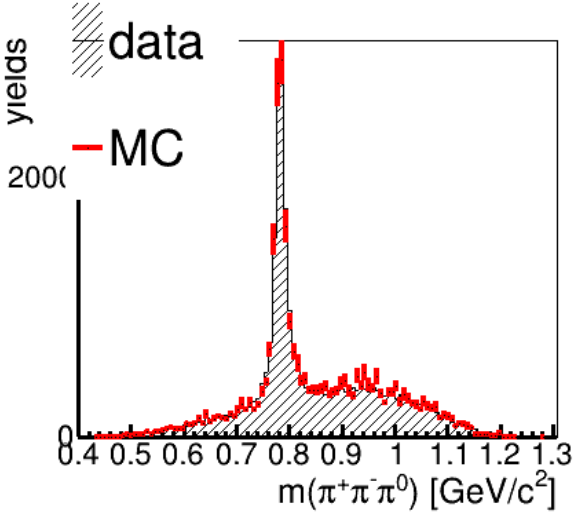
data
MC
yields
200(
0
0.4 0.5 0.6 0.7 0.8 0.9 1 1.1 1.2 1.3
$m(\pi^+\pi^-\pi^0)$ [GeV/c^2]

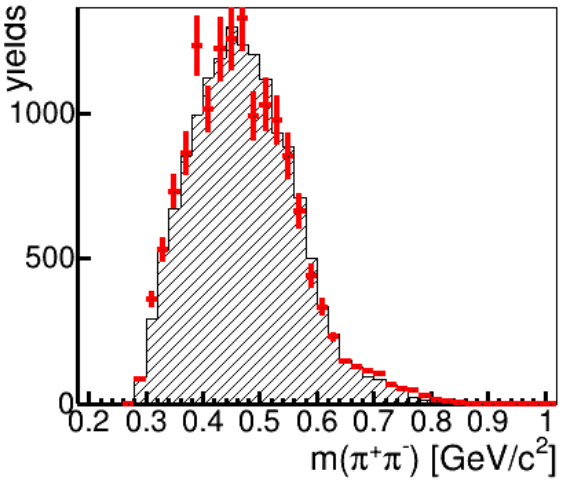
yields
1000
500
0
0.2 0.3 0.4 0.5 0.6 0.7 0.8 0.9 1
$m(\pi^+\pi^-)$ [GeV/c^2]

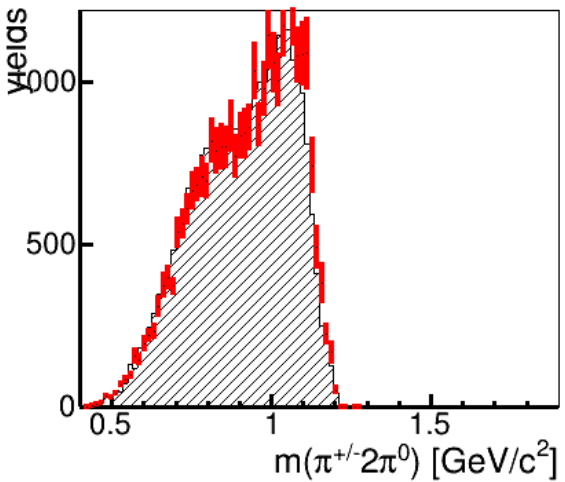
yields
000
500
0
0.5
1
1.5
$m(\pi^{+/-}2\pi^0)$ [GeV/c^2]

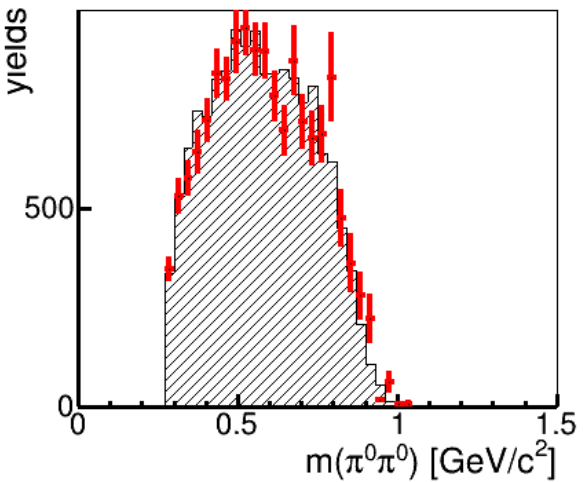
yields
500
0
0
0.5
1
1.5
$m(\pi^0\pi^0)$ [GeV/c^2]

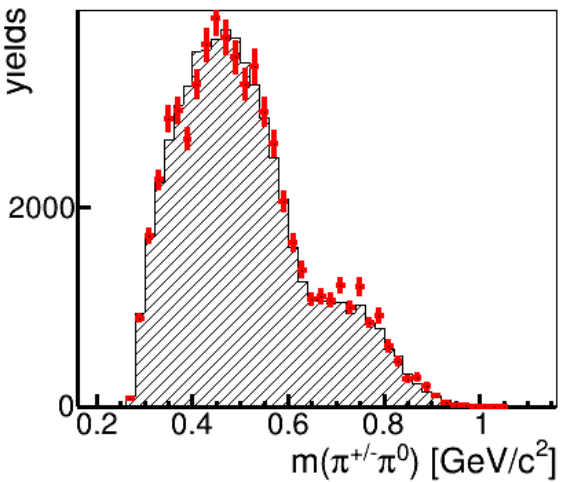
yields
2000
0
0.2
0.4
0.6
0.8
1
$m(\pi^{+/-}\pi^0)$ [GeV/c^2]

(ee → pi⁺pi⁻2pi⁰)

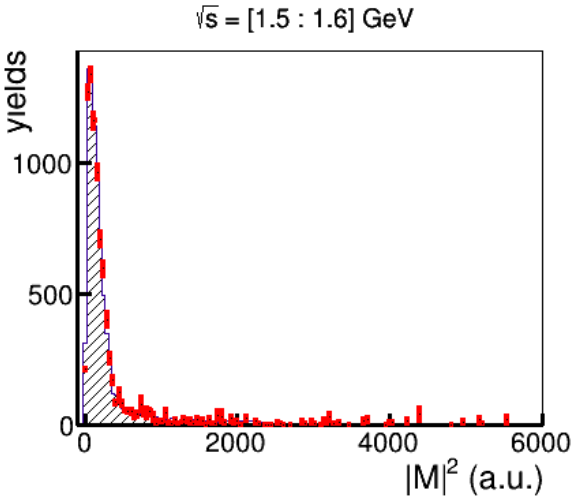
√s = [1.5 : 1.6] GeV
yields
1000
500
0
0
2000
4000
6000
|M|² (a.u.)

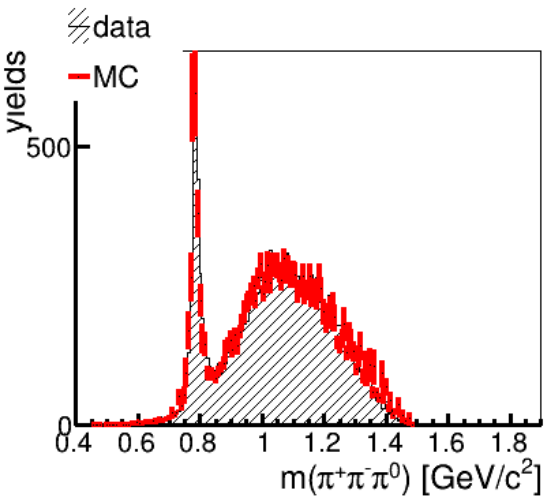
data
MC
yields
500
0
0.4
0.6
0.8
1
1.2
1.4
1.6
1.8
m(π⁺π⁻π⁰) [GeV/c²]

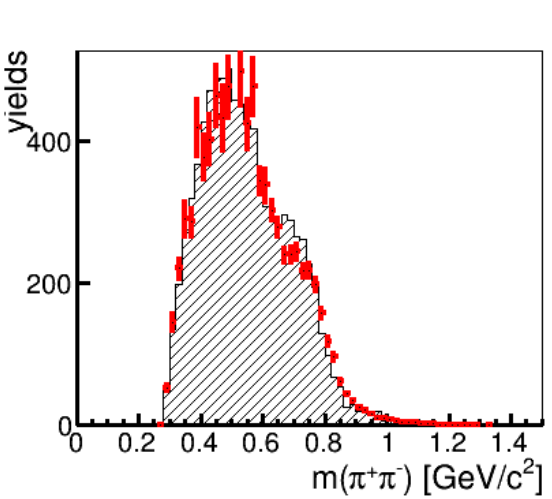
yields
400
200
0
0
0.2
0.4
0.6
0.8
1
1.2
1.4
m(π⁺π⁻) [GeV/c²]

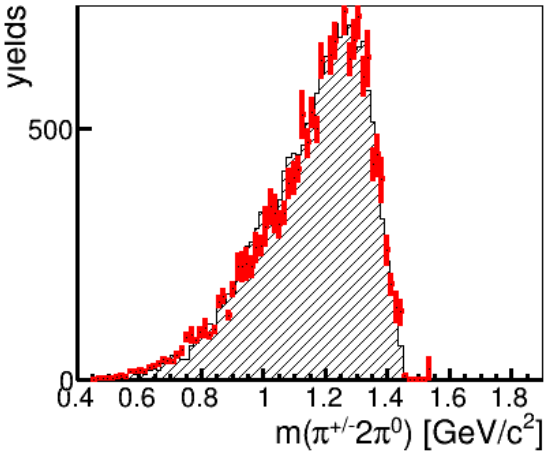
yields
500
0
0.4
0.6
0.8
1
1.2
1.4
1.6
1.8
m(π⁺/⁻2π⁰) [GeV/c²]

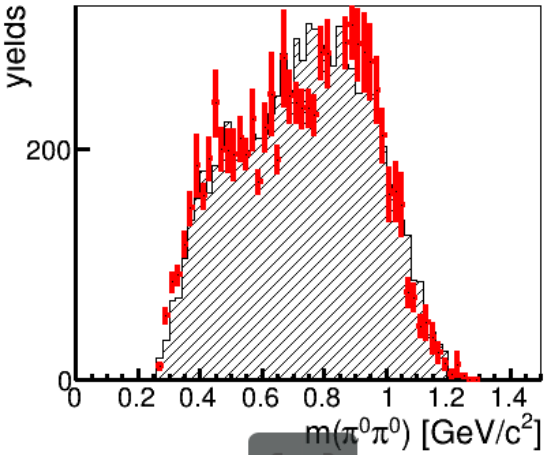
yields
200
0
0
0.2
0.4
0.6
0.8
1
1.2
1.4
m(π⁰π⁰) [GeV/c²]

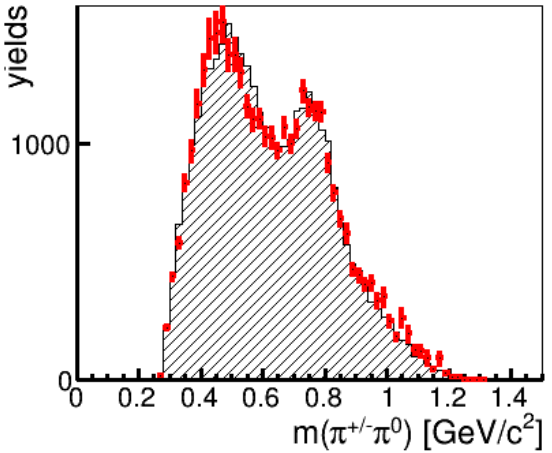
yields
1000
0
0
0.2
0.4
0.6
0.8
1
1.2
1.4
m(π⁺/⁻π⁰) [GeV/c²]

(ee → $\pi^+\pi^-2\pi^0$)

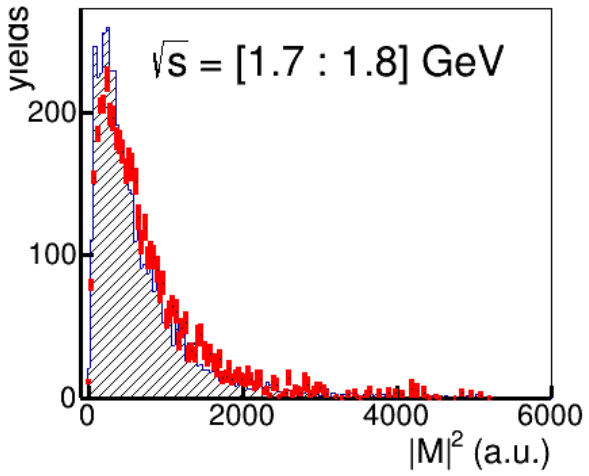
yields
$\sqrt{s}$ = [1.7 : 1.8] GeV
$|M|^2$ (a.u.)

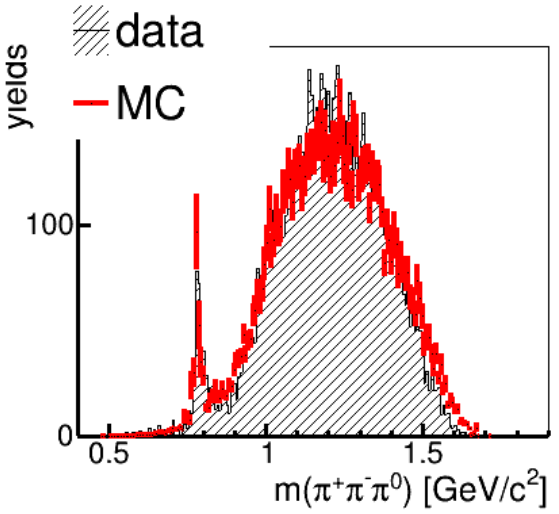
data
MC
yields
$m(\pi^+\pi^-\pi^0)$ [GeV/c^2]

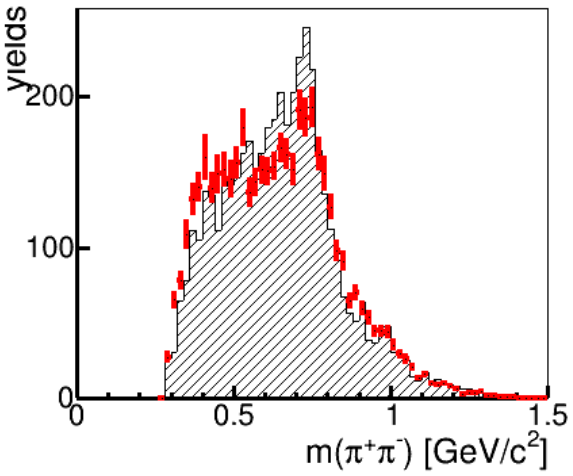
yields
$m(\pi^+\pi^-)$ [GeV/c^2]

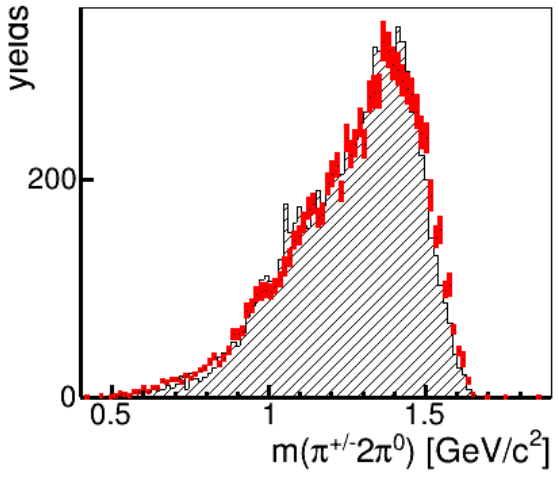
yields
$m(\pi^{+/-}2\pi^0)$ [GeV/c^2]

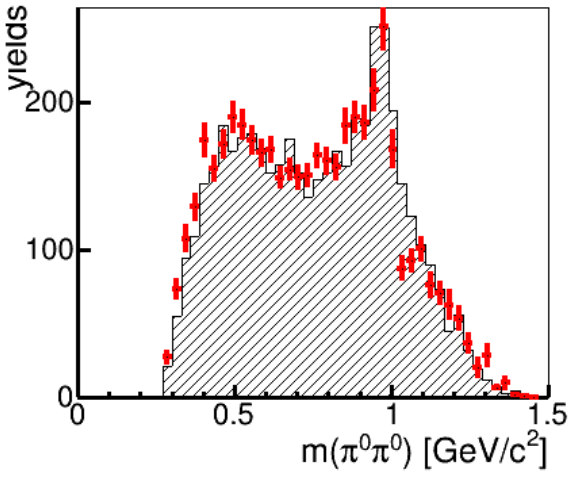
yields
$m(\pi^0\pi^0)$ [GeV/c^2]

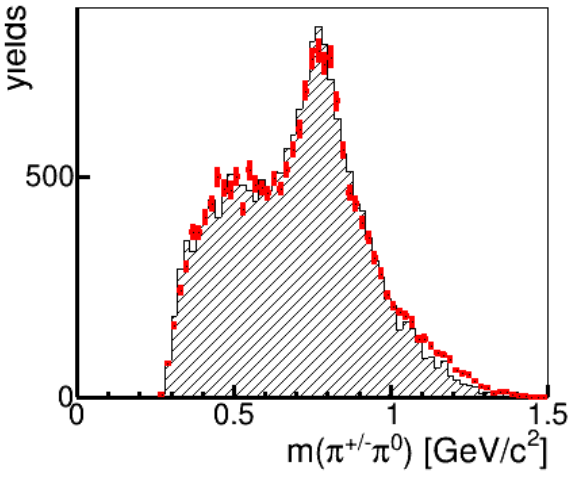
yields
$m(\pi^{+/-}\pi^0)$ [GeV/c^2]

(ee → $\pi^+\pi^-2\pi^0$)

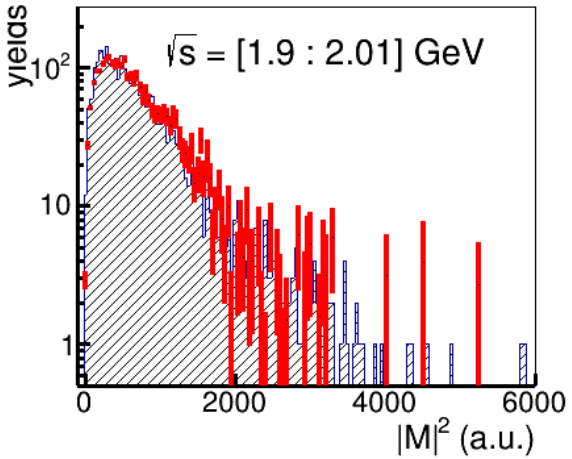
yields
$\sqrt{s}$ = [1.9 : 2.01] GeV
$|M|^2$ (a.u.)

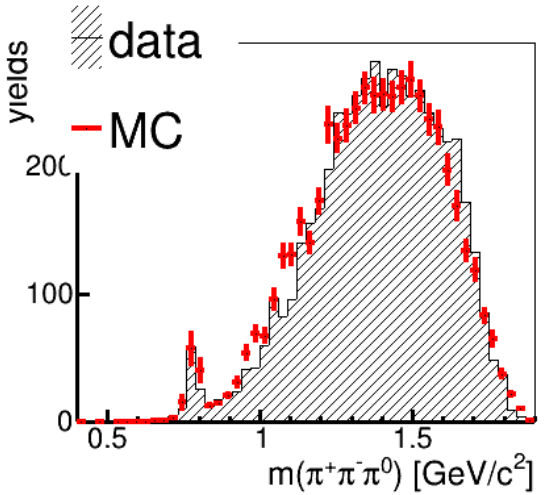
data
MC
yields
$m(\pi^+\pi^-\pi^0)$ [GeV/c^2]

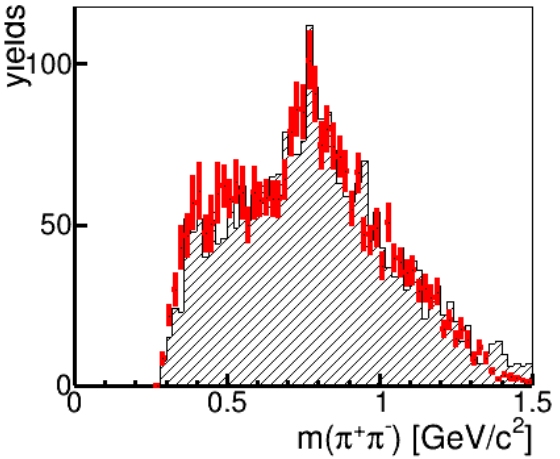
yields
$m(\pi^+\pi^-)$ [GeV/c^2]

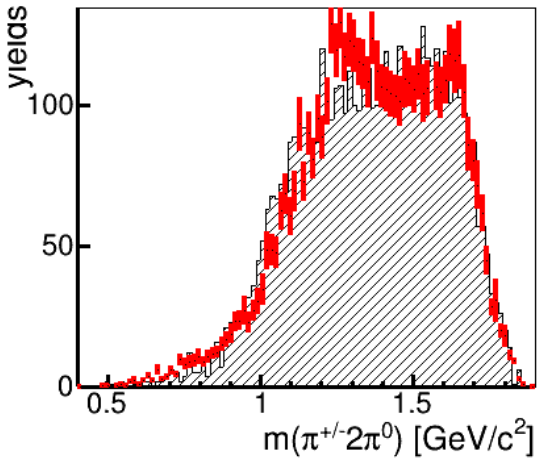
yields
$m(\pi^{+/-}2\pi^0)$ [GeV/c^2]

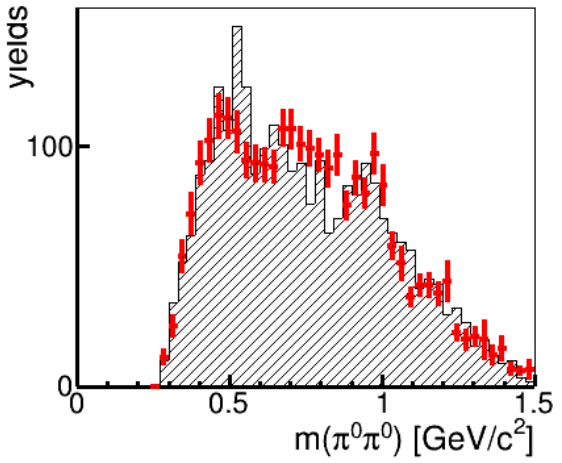
yields
$m(\pi^0\pi^0)$ [GeV/c^2]

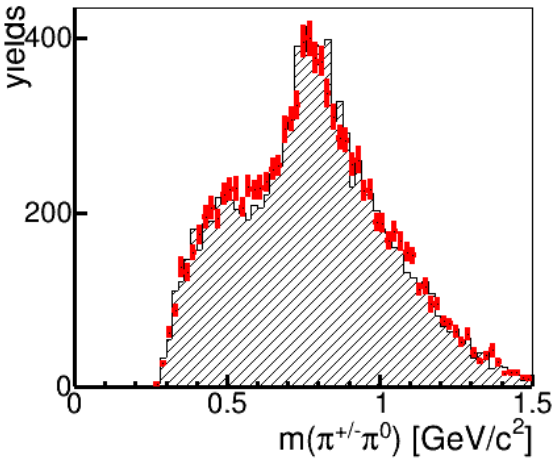
yields
$m(\pi^{+/-}\pi^0)$ [GeV/c^2]

(ee → 2pi⁺2pi⁻)

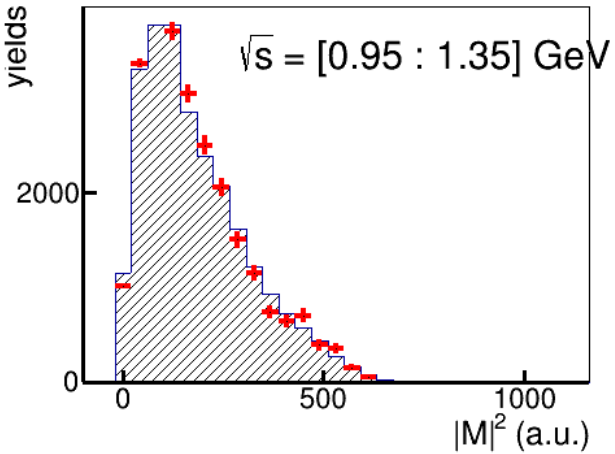
yields
√s = [0.95 : 1.35] GeV
2000
0
0
500
1000
|M|² (a.u.)

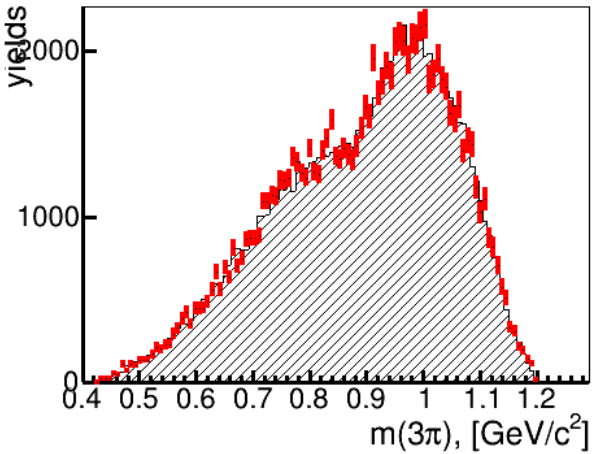
yields
2000
1000
0
0.4 0.5 0.6 0.7 0.8 0.9 1 1.1 1.2
m(3π), [GeV/c²]

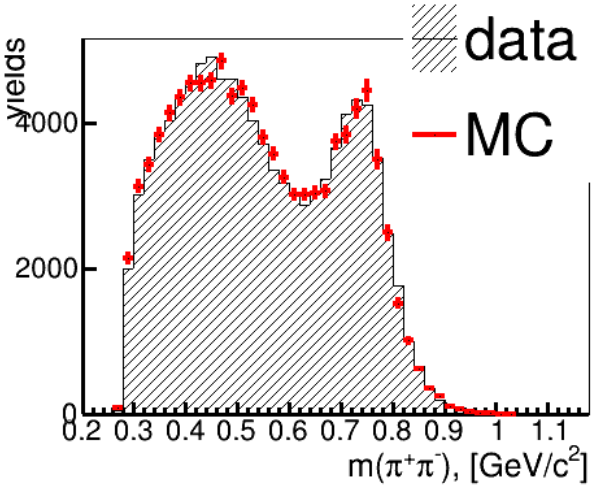
yields
data
MC
4000
2000
0
0.2 0.3 0.4 0.5 0.6 0.7 0.8 0.9 1 1.1
m(π⁺π⁻), [GeV/c²]

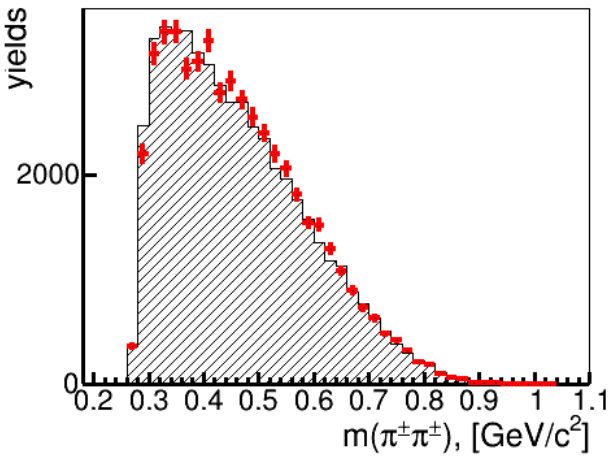
yields
2000
0
0.2 0.3 0.4 0.5 0.6 0.7 0.8 0.9 1 1.1
m(π±π±), [GeV/c²]

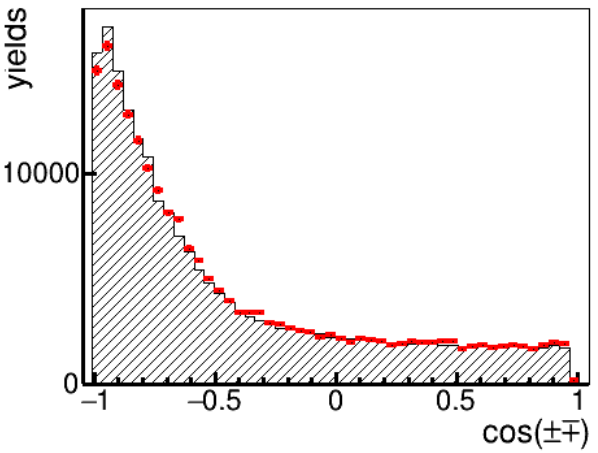
yields
10000
0
–1 –0.5 0 0.5 1
cos(±∓)

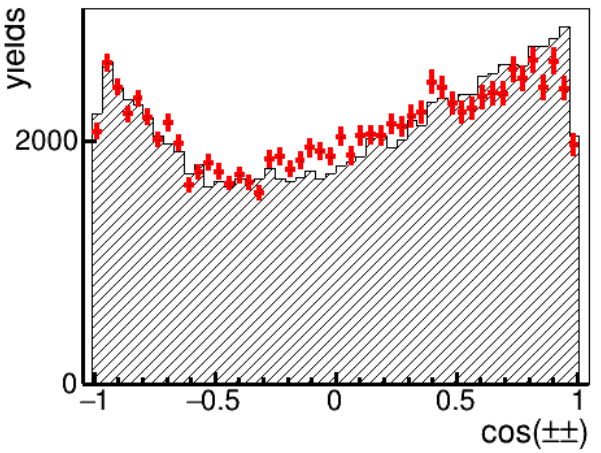
yields
2000
0
–1 –0.5 0 0.5 1
cos(±±)

(ee → 2pi⁺2pi⁻)

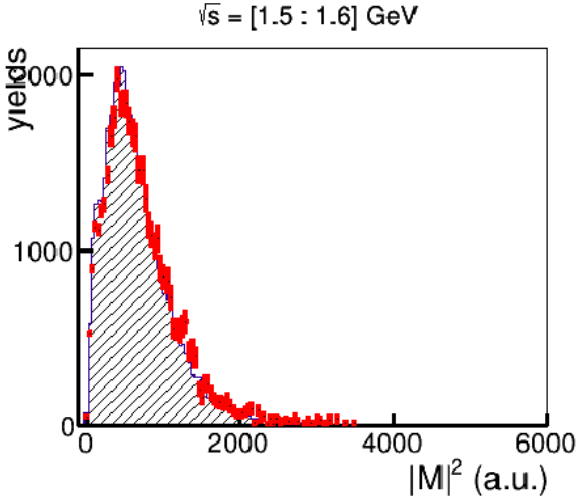
√s = [1.5 : 1.6] GeV
yields
|M|² (a.u.)

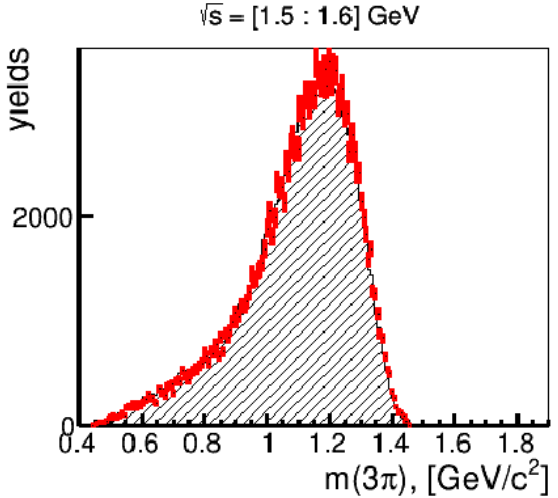
√s = [1.5 : 1.6] GeV
yields
m(3π), [GeV/c²]

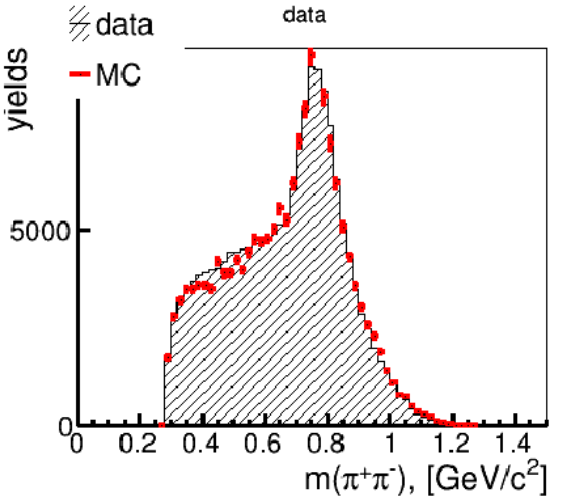
data
MC
data
yields
m(π⁺π⁻), [GeV/c²]

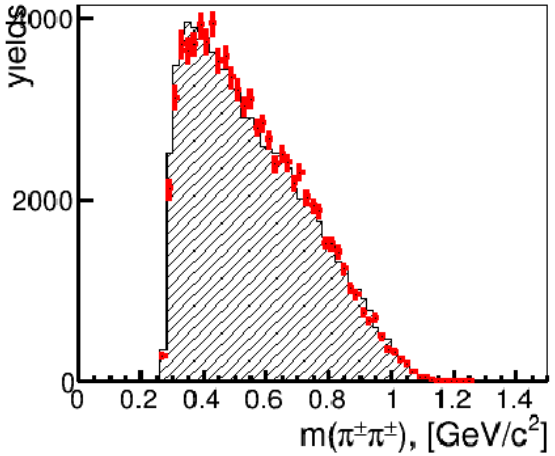
yields
m(π±π±), [GeV/c²]

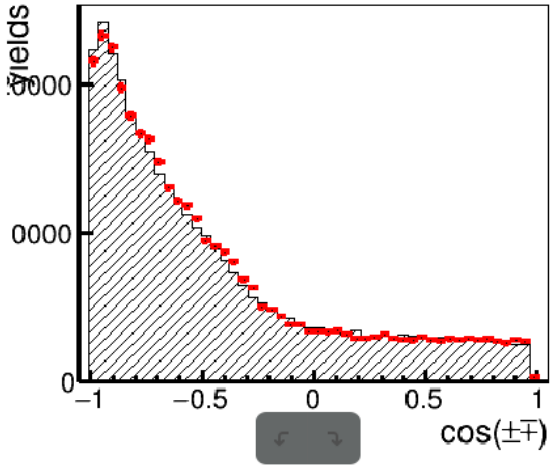
yields
cos(±∓)

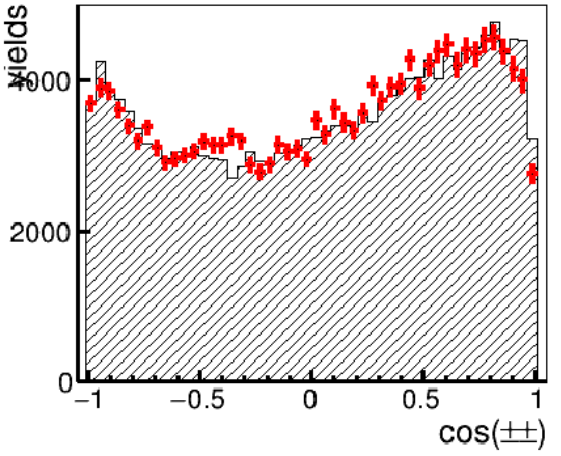
yields
cos(±±)

(ee → 2pi⁺2pi⁻)

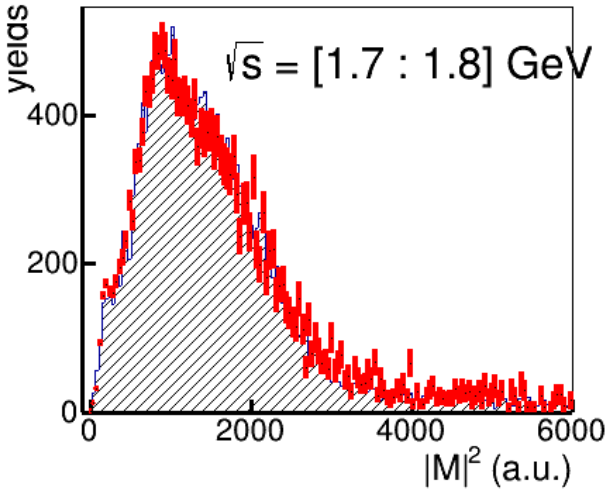
yields
√s = [1.7 : 1.8] GeV
400
200
0
0
2000
4000
6000
|M|² (a.u.)

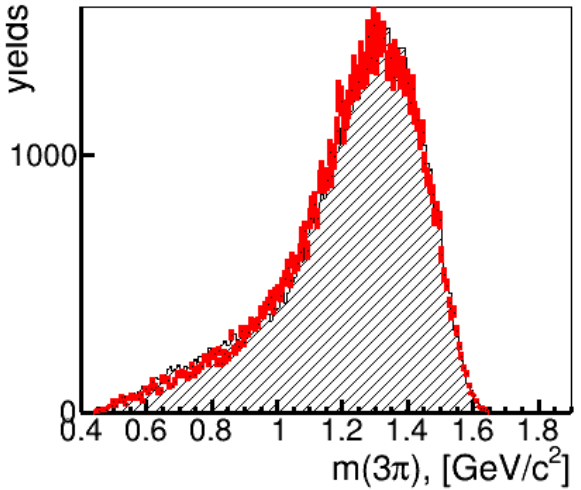
yields
1000
0
0.4
0.6
0.8
1
1.2
1.4
1.6
1.8
m(3π), [GeV/c²]

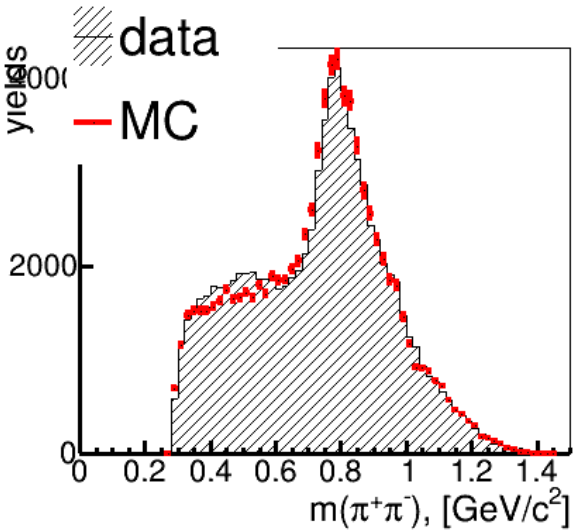
data
MC
yields
2000
0
0
0.2
0.4
0.6
0.8
1
1.2
1.4
m(π⁺π⁻), [GeV/c²]

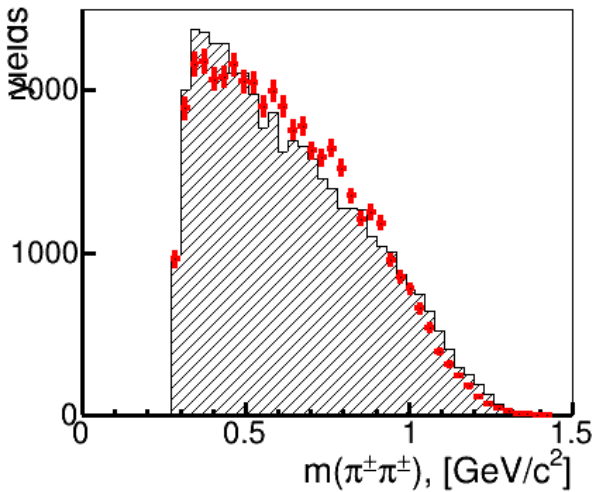
yields
1000
0
0
0.5
1
1.5
m(π±π±), [GeV/c²]

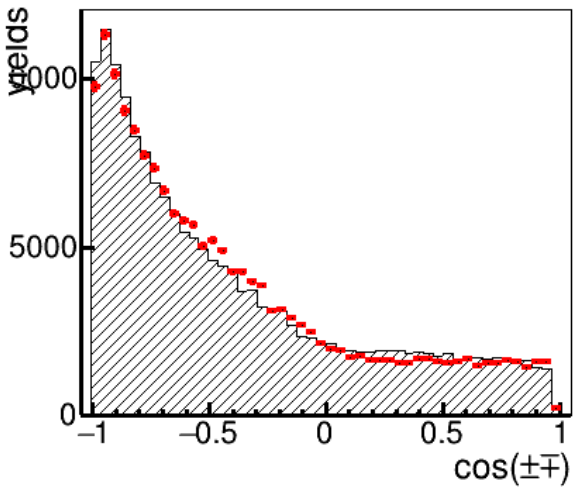
yields
5000
0
–1
–0.5
0
0.5
1
cos(±∓)

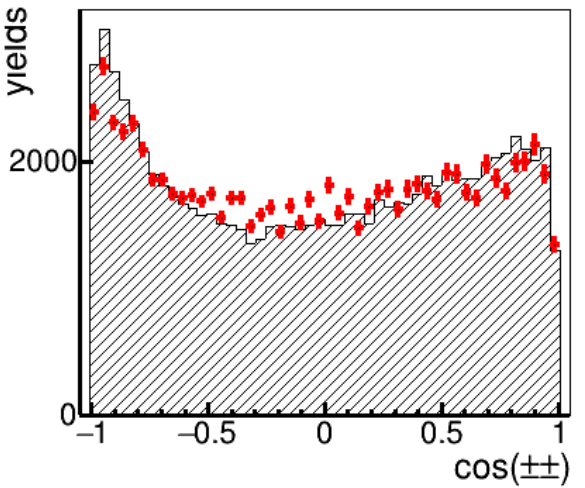
yields
2000
0
–1
–0.5
0
0.5
1
cos(±±)

(ee → 2pi⁺2pi⁻)

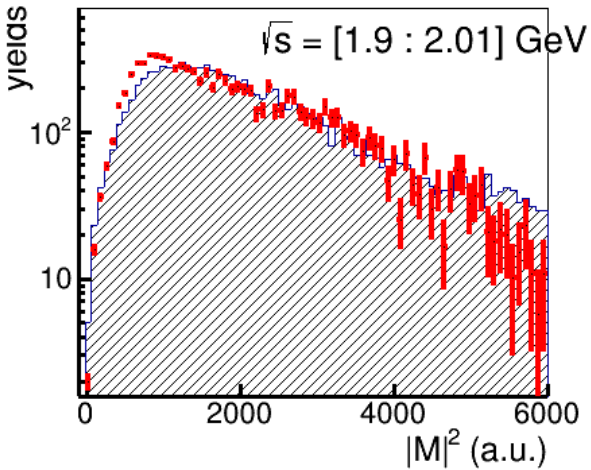
yields
√s = [1.9 : 2.01] GeV
10^2
10
0
2000
4000
6000
$|M|^2$ (a.u.)

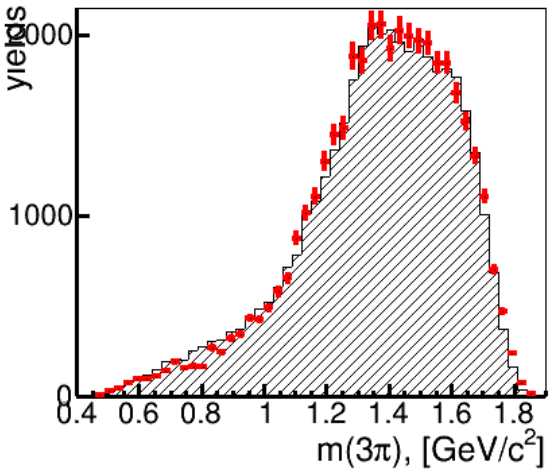
yields
2000
1000
0
0.4
0.6
0.8
1
1.2
1.4
1.6
1.8
m(3π), [GeV/c²]

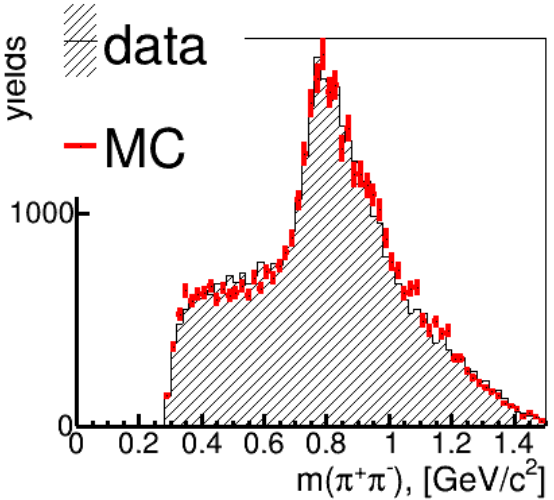
yields
data
MC
1000
0
0.2
0.4
0.6
0.8
1
1.2
1.4
m(π⁺π⁻), [GeV/c²]

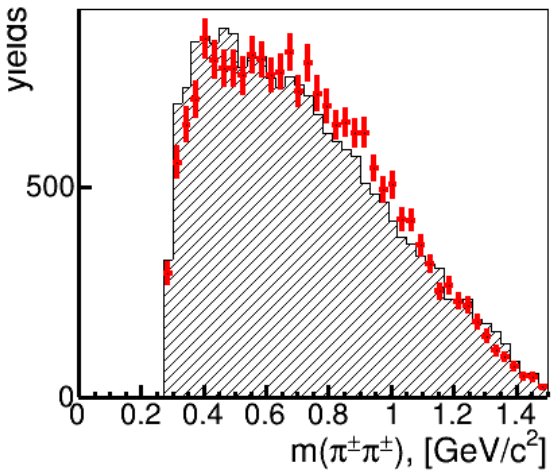
yields
500
0
0.2
0.4
0.6
0.8
1
1.2
1.4
m(π±π±), [GeV/c²]

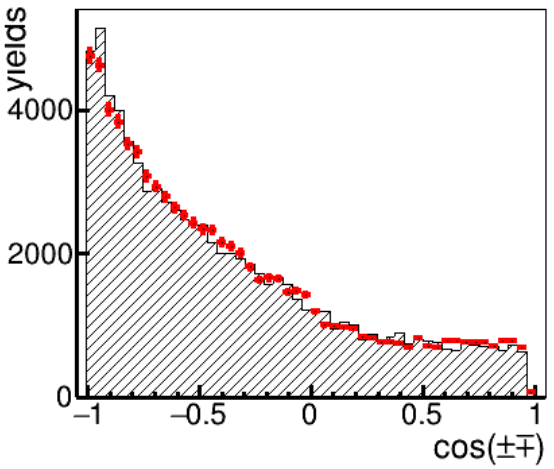
yields
4000
2000
0
−1
−0.5
0
0.5
1
cos(±∓)

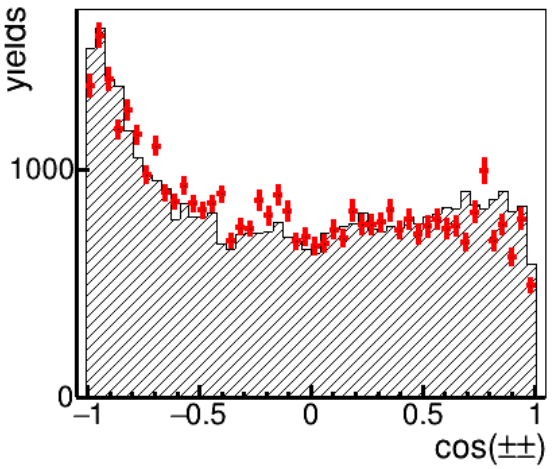
yields
1000
0
−1
−0.5
0
0.5
1
cos(±±)

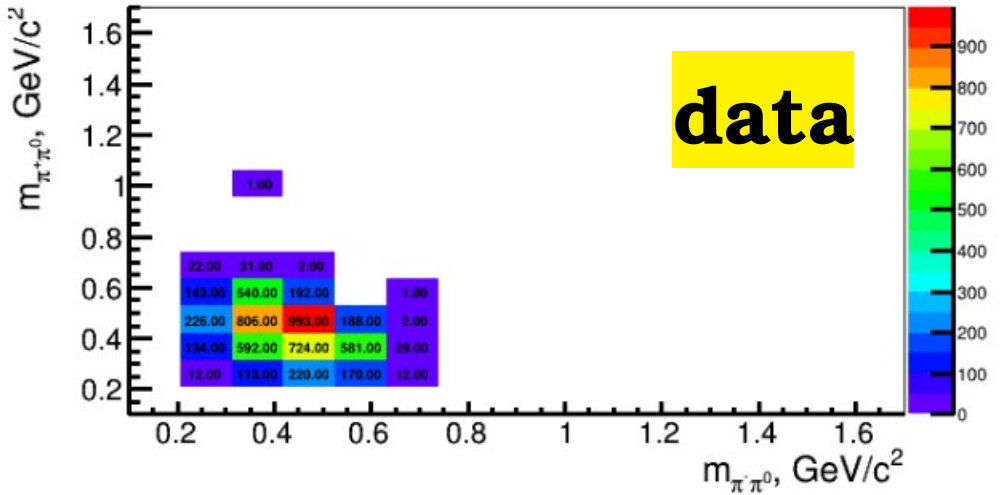
data
$m_{\pi^+\pi^0}$, GeV/c^2
$m_{\pi^-\pi^0}$, GeV/c^2

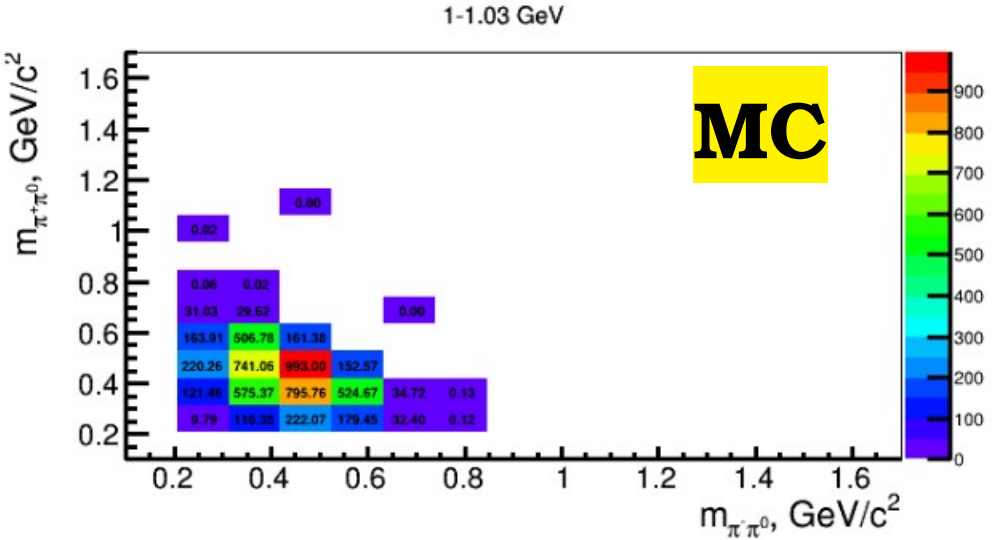
1-1.03 GeV
MC
$m_{\pi^+\pi^0}$, GeV/c^2
$m_{\pi^-\pi^0}$, GeV/c^2

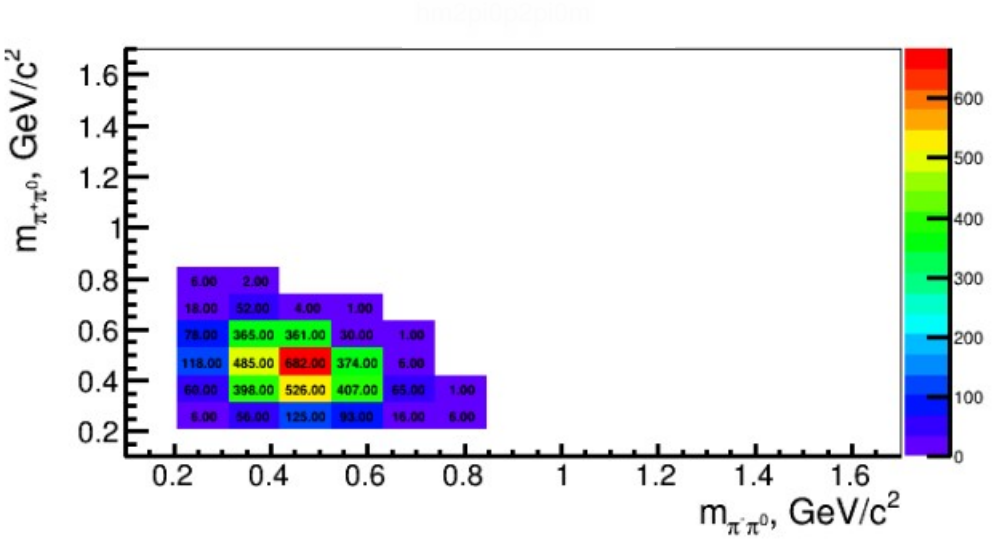
$m_{\pi^+\pi^0}$, GeV/c^2
$m_{\pi^-\pi^0}$, GeV/c^2

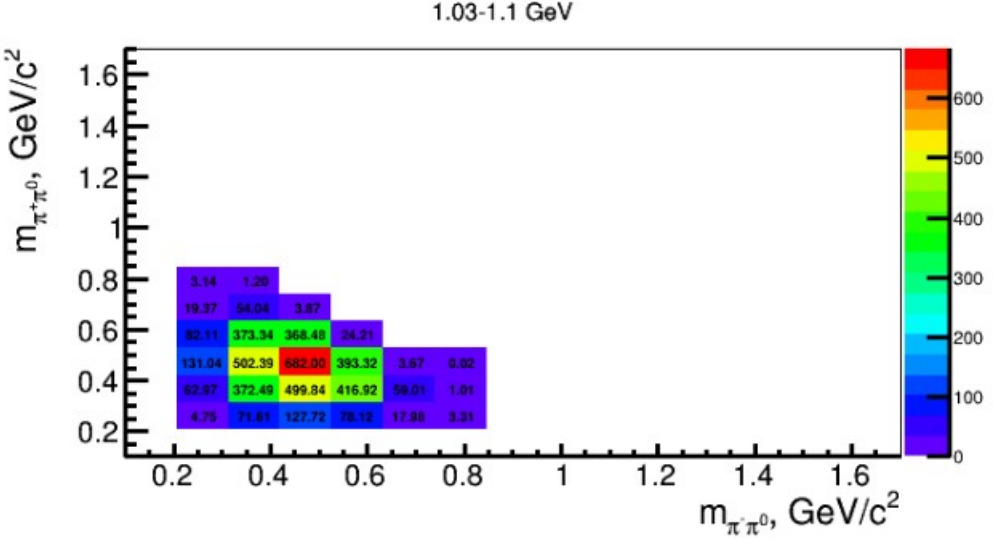
1.03-1.1 GeV
$m_{\pi^+\pi^0}$, GeV/c^2
$m_{\pi^-\pi^0}$, GeV/c^2

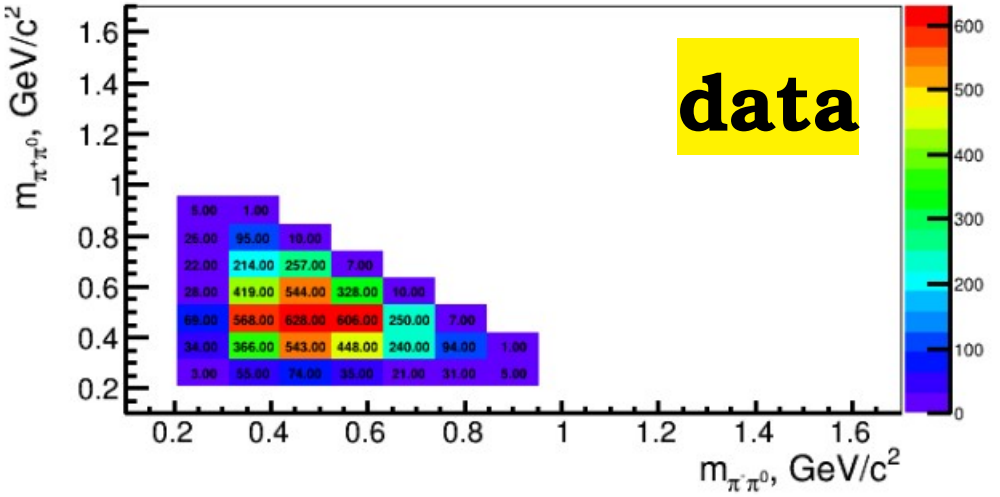
data
$m_{\pi^+\pi^0}$, GeV/c^2
$m_{\pi^-\pi^0}$, GeV/c^2

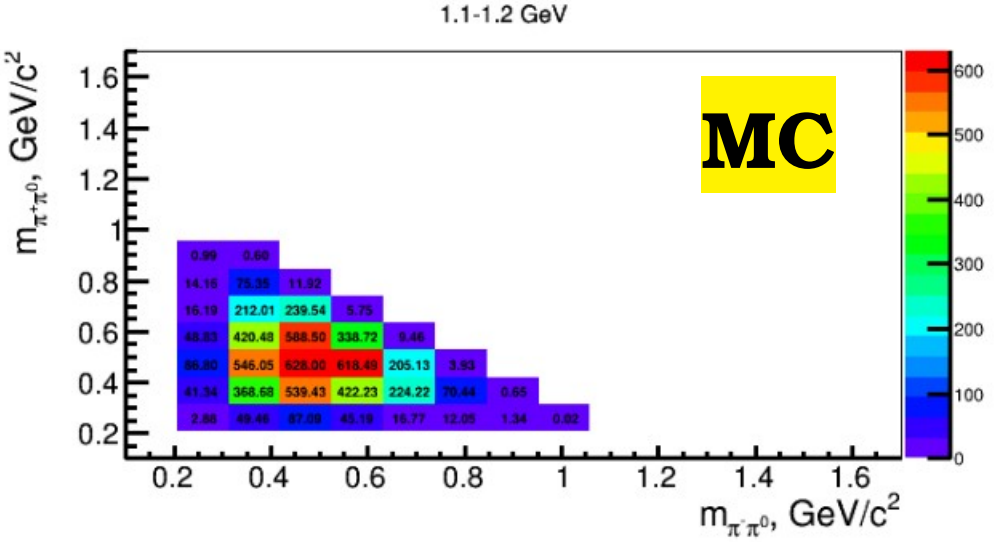
1.1-1.2 GeV
MC
$m_{\pi^+\pi^0}$, GeV/c^2
$m_{\pi^-\pi^0}$, GeV/c^2

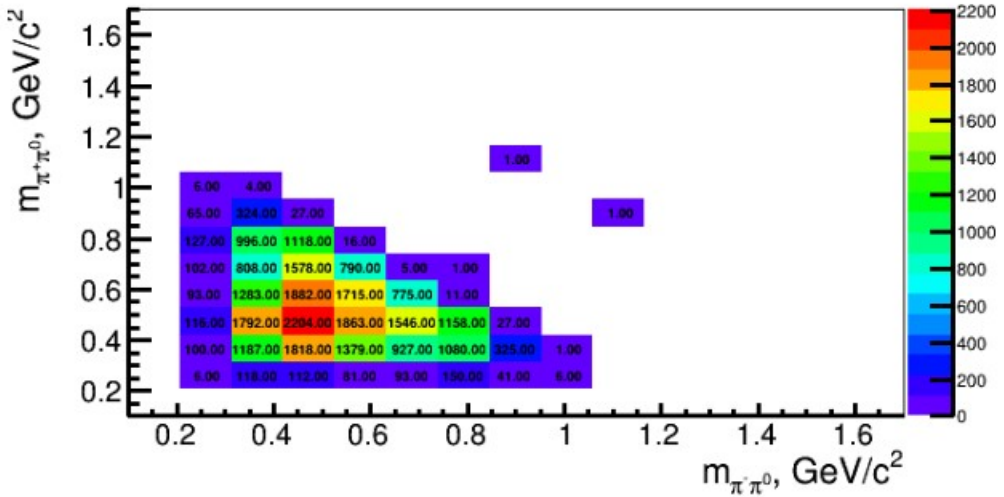
$m_{\pi^+\pi^0}$, GeV/c^2
$m_{\pi^-\pi^0}$, GeV/c^2

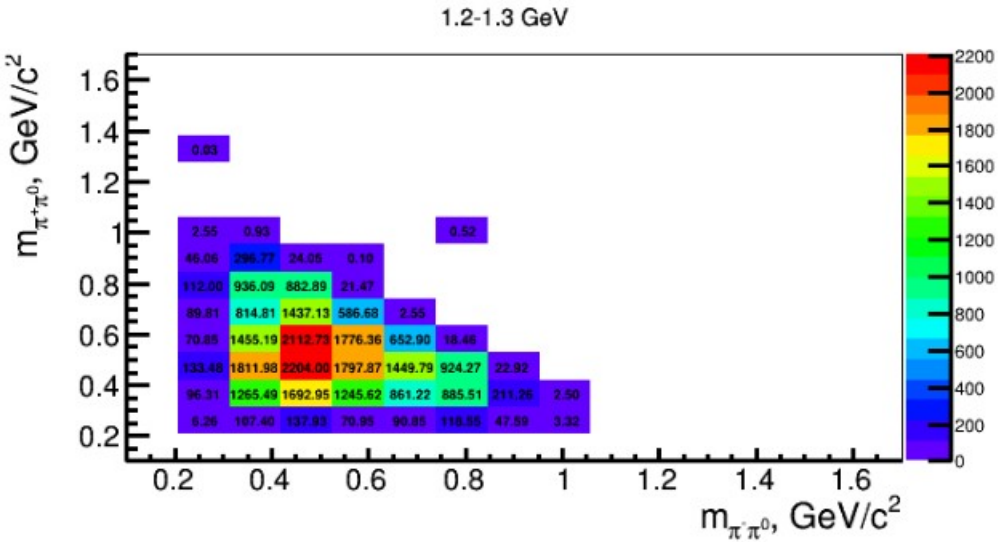
1.2-1.3 GeV
$m_{\pi^+\pi^0}$, GeV/c^2
$m_{\pi^-\pi^0}$, GeV/c^2

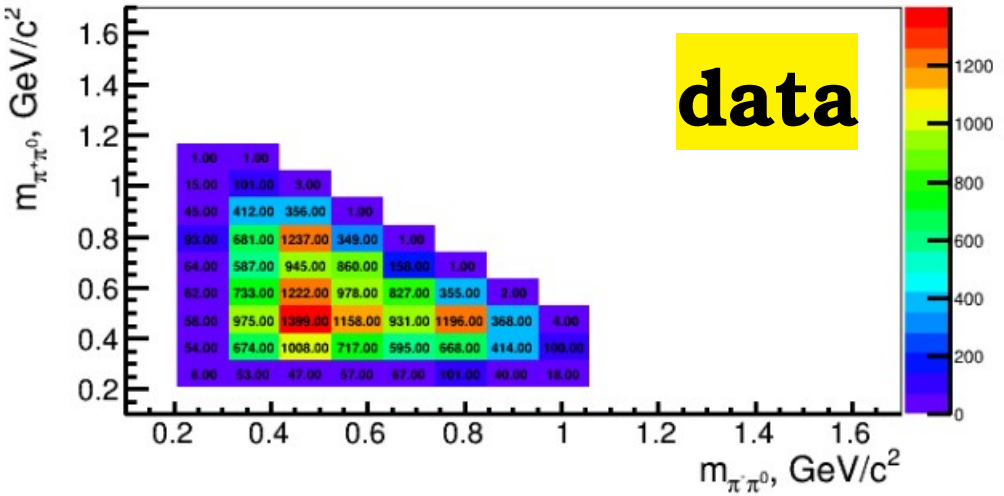
data
$m_{\pi^+\pi^0}$, GeV/c^2
$m_{\pi^-\pi^0}$, GeV/c^2

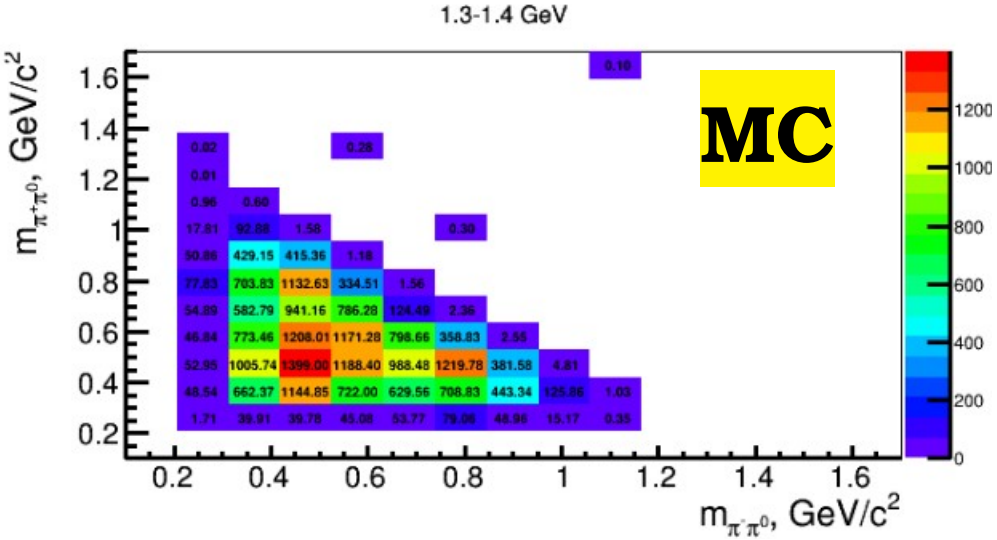
1.3-1.4 GeV
MC
$m_{\pi^+\pi^0}$, GeV/c^2
$m_{\pi^-\pi^0}$, GeV/c^2

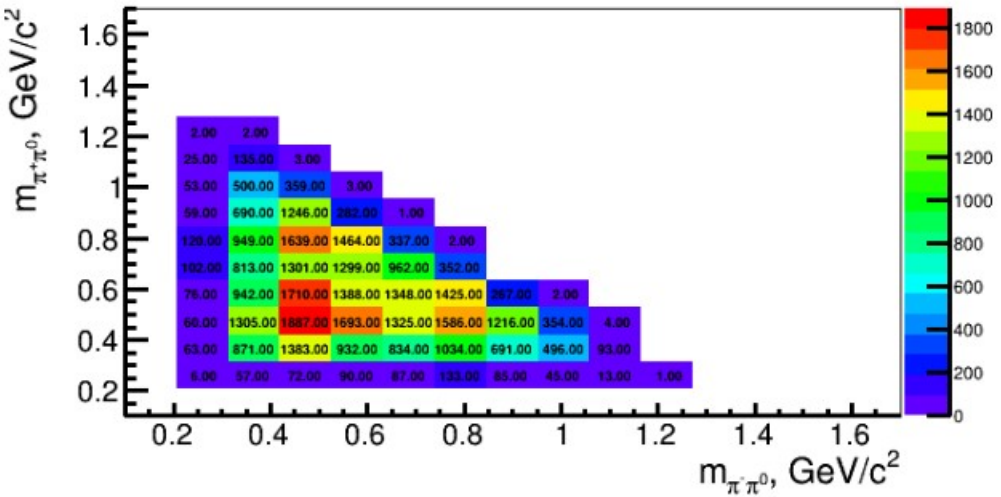
$m_{\pi^+\pi^0}$, GeV/c^2
$m_{\pi^-\pi^0}$, GeV/c^2

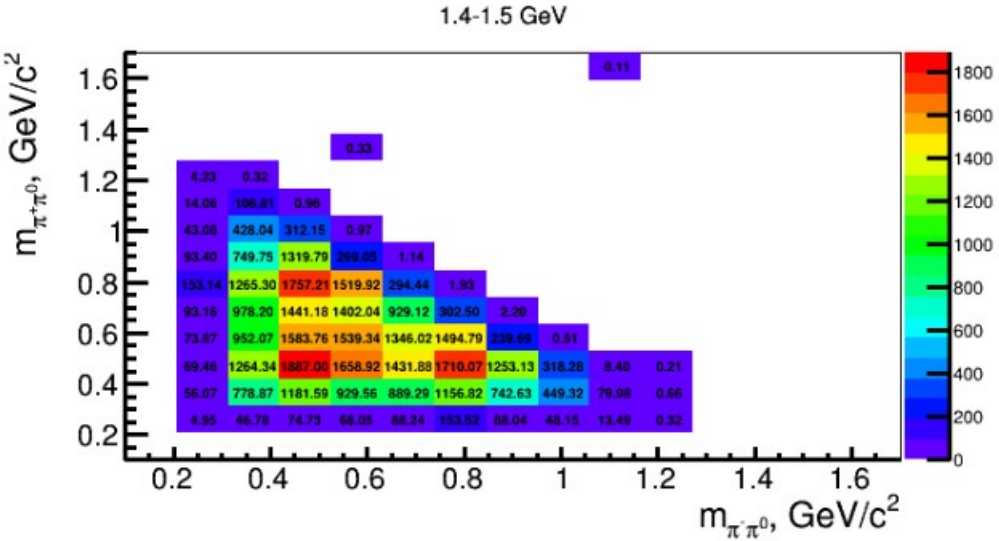
1.4-1.5 GeV
$m_{\pi^+\pi^0}$, GeV/c^2
$m_{\pi^-\pi^0}$, GeV/c^2

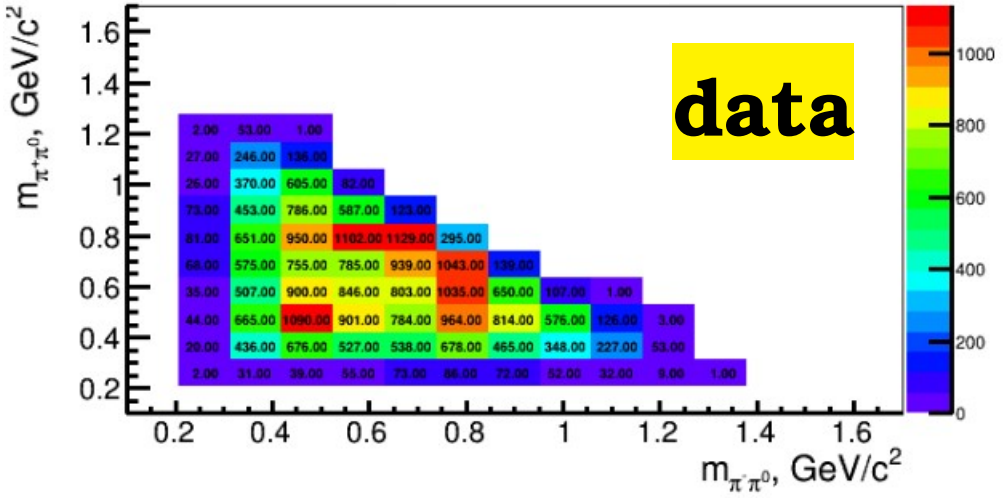
data
$m_{\pi^+\pi^0}$, GeV/c^2
$m_{\pi^-\pi^0}$, GeV/c^2

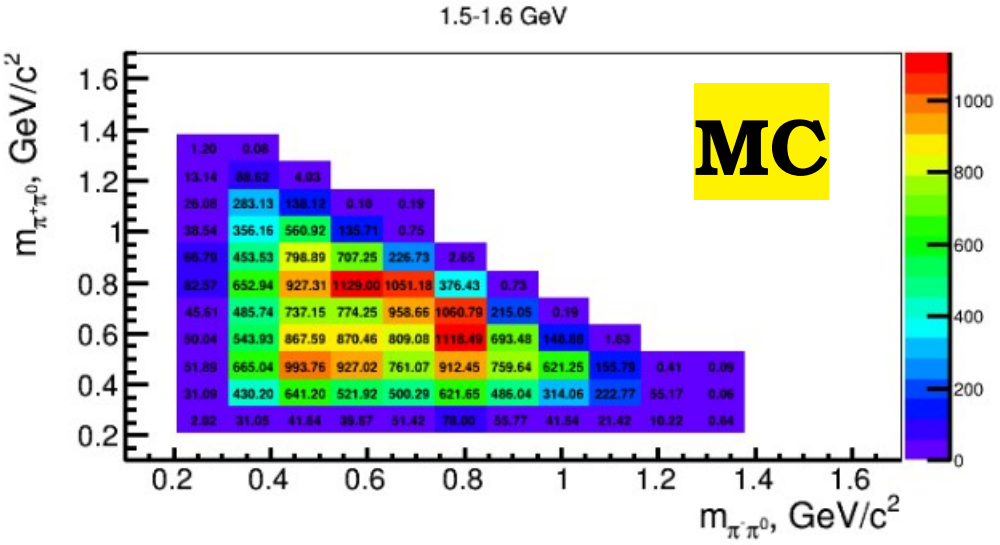
1.5-1.6 GeV
MC
$m_{\pi^+\pi^0}$, GeV/c^2
$m_{\pi^-\pi^0}$, GeV/c^2

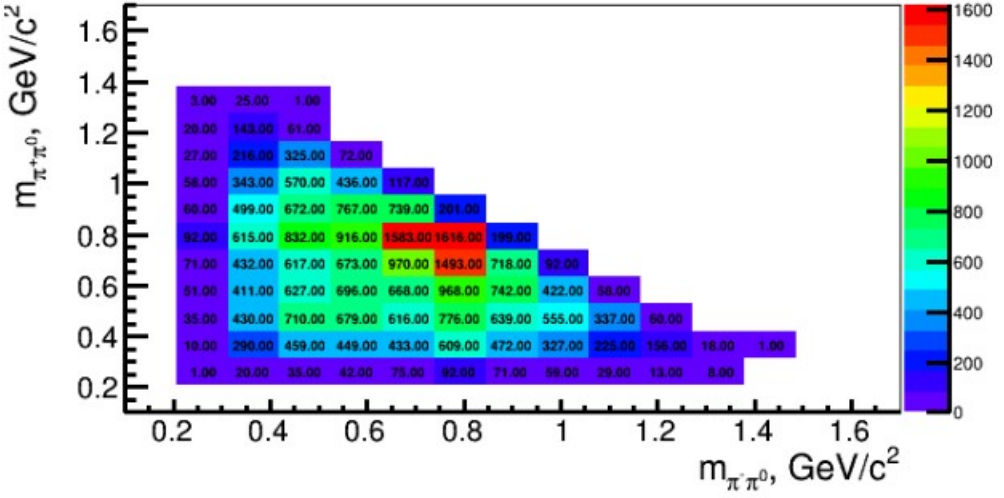
$m_{\pi^+\pi^0}$, GeV/c^2
$m_{\pi^-\pi^0}$, GeV/c^2

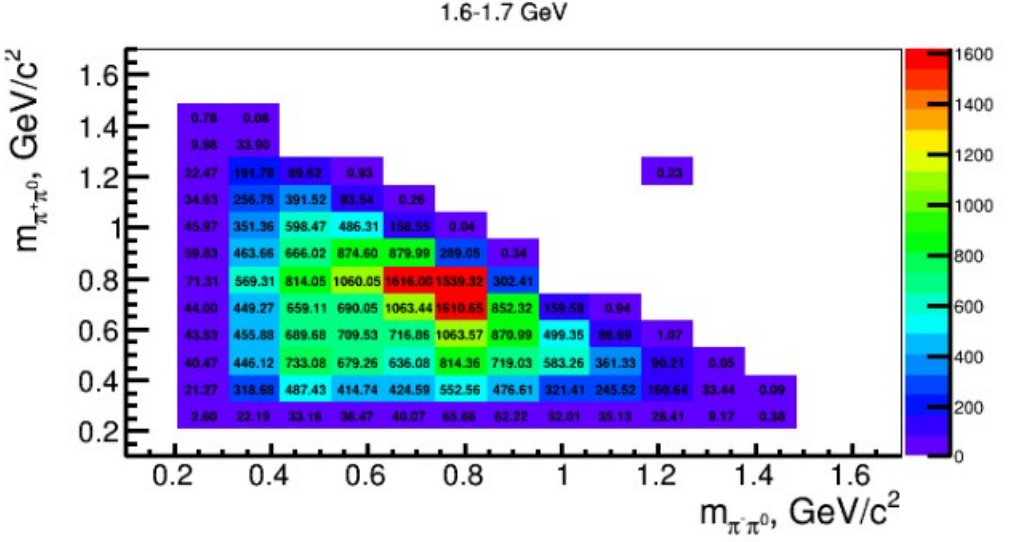
1.6-1.7 GeV
$m_{\pi^+\pi^0}$, GeV/c^2
$m_{\pi^-\pi^0}$, GeV/c^2

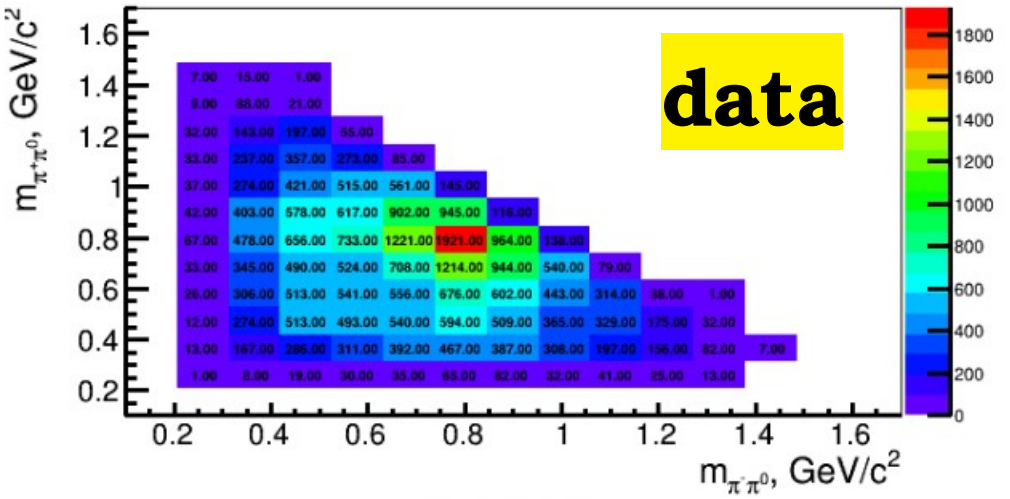
data
$m_{\pi^+\pi^0}$, GeV/c^2
$m_{\pi^-\pi^0}$, GeV/c^2

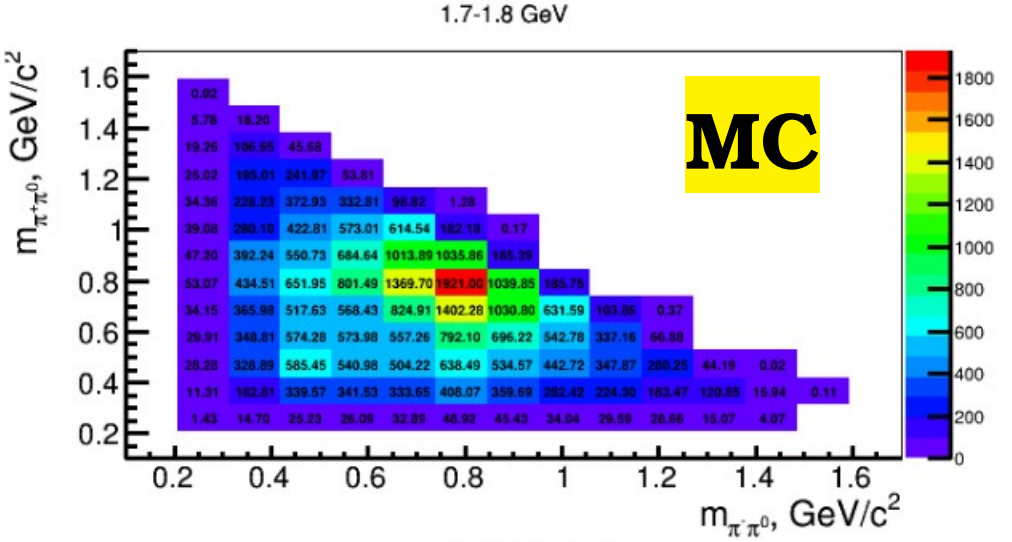
1.7-1.8 GeV
MC
$m_{\pi^+\pi^0}$, GeV/c^2
$m_{\pi^-\pi^0}$, GeV/c^2

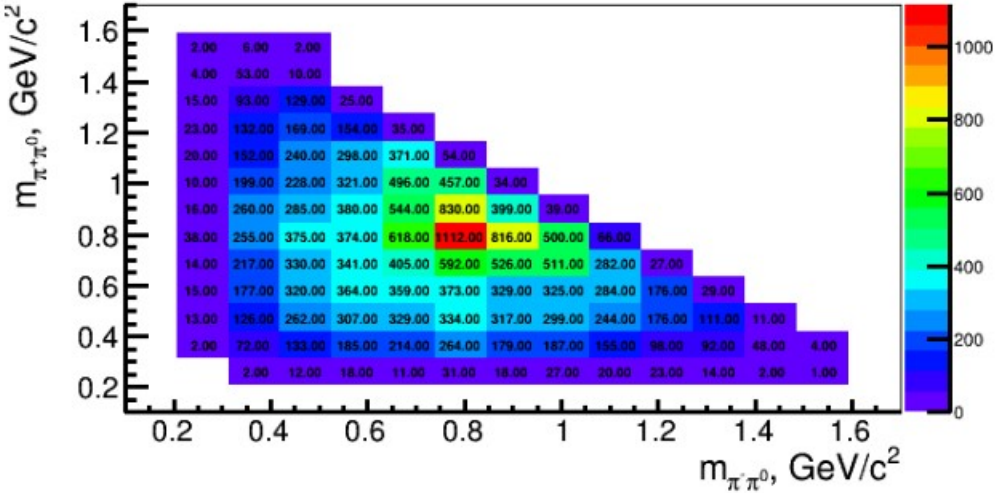
$m_{\pi^+\pi^0}$, GeV/c^2
$m_{\pi^-\pi^0}$, GeV/c^2

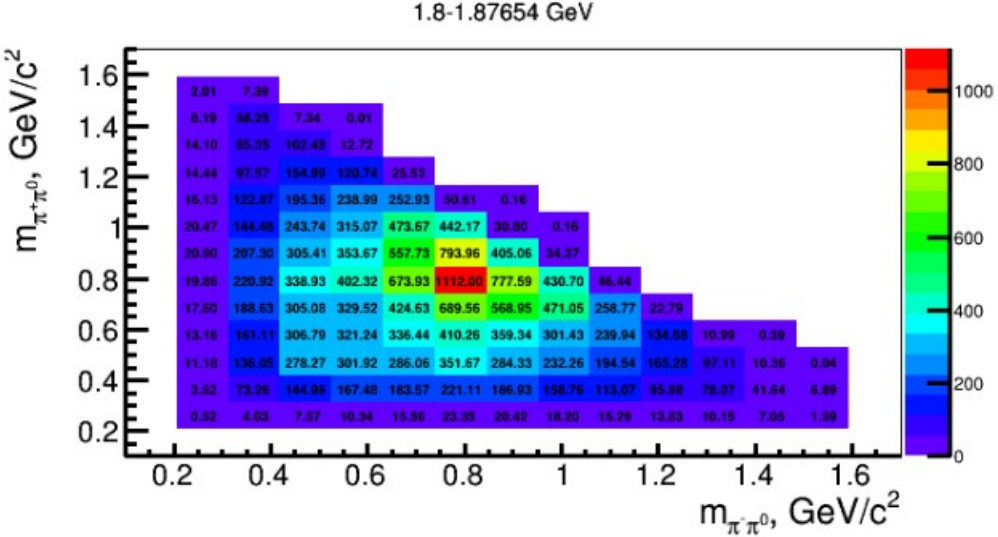
1.8-1.87654 GeV
$m_{\pi^+\pi^0}$, GeV/c^2
$m_{\pi^-\pi^0}$, GeV/c^2

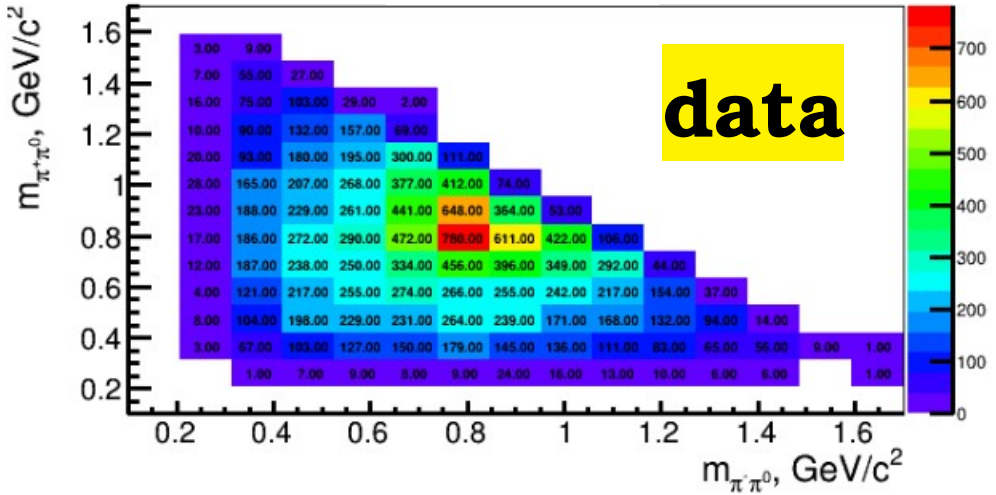
data
$m_{\pi^+\pi^0}$, GeV/c^2
$m_{\pi^-\pi^0}$, GeV/c^2

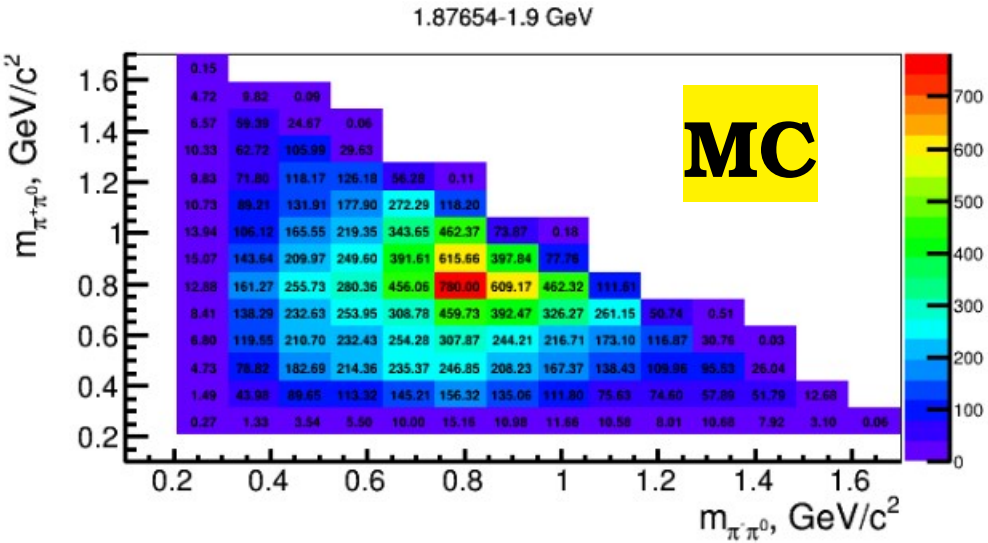
1.87654-1.9 GeV
MC
$m_{\pi^+\pi^0}$, GeV/c^2
$m_{\pi^-\pi^0}$, GeV/c^2

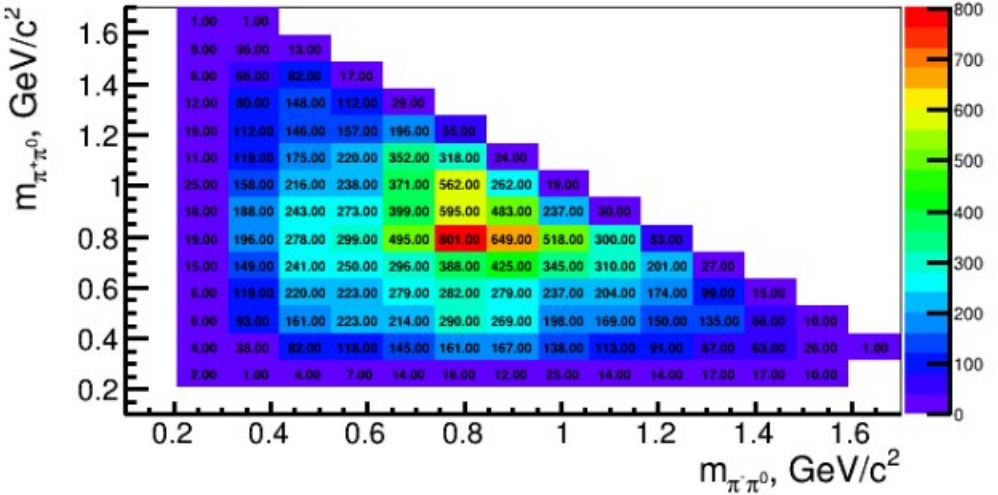
$m_{\pi^+\pi^0}$, GeV/c^2
$m_{\pi^-\pi^0}$, GeV/c^2

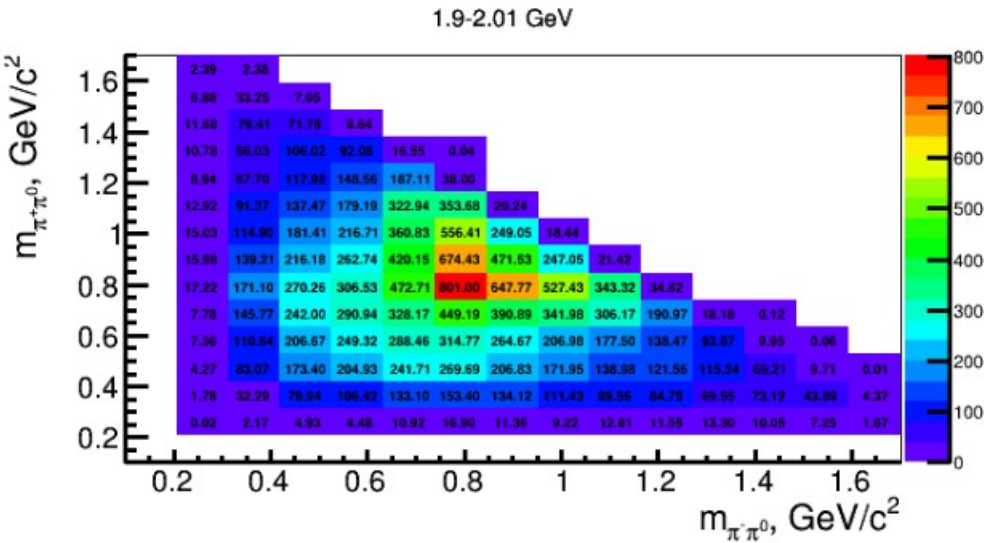
1.9-2.01 GeV
$m_{\pi^+\pi^0}$, GeV/c^2
$m_{\pi^-\pi^0}$, GeV/c^2

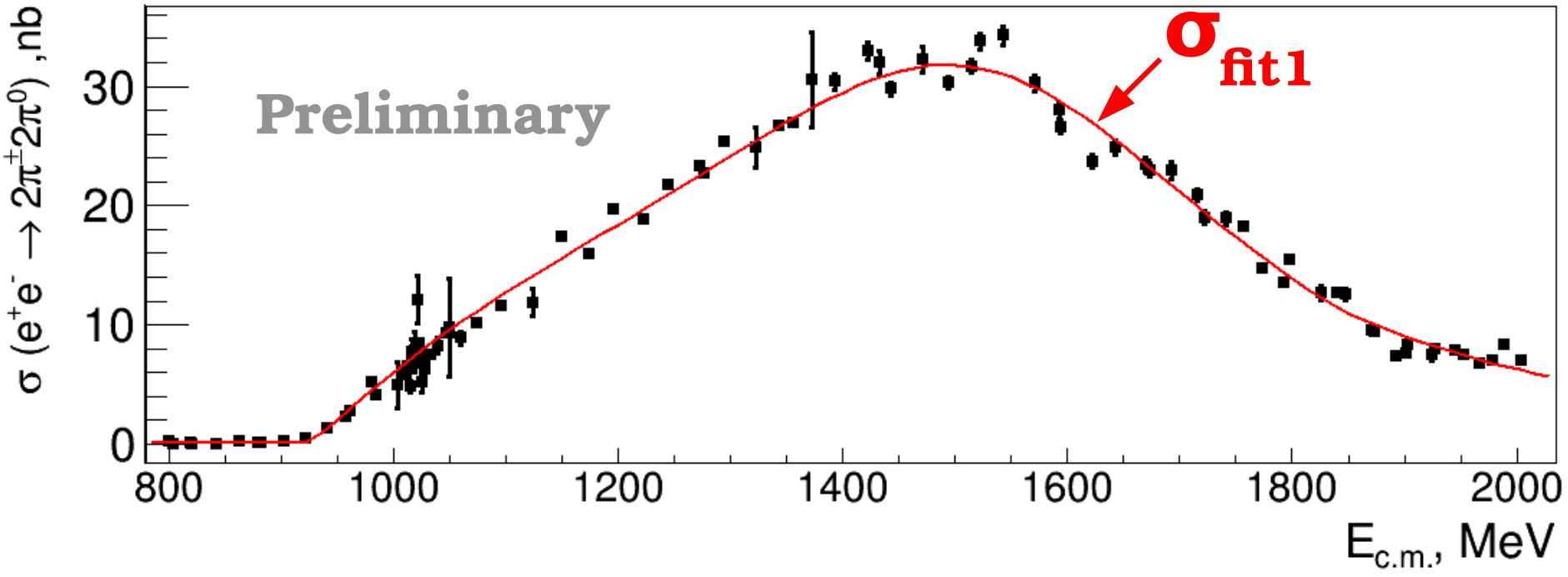

The cross-section of e+e- → π+π-2π0 obtained by using the model described above

results

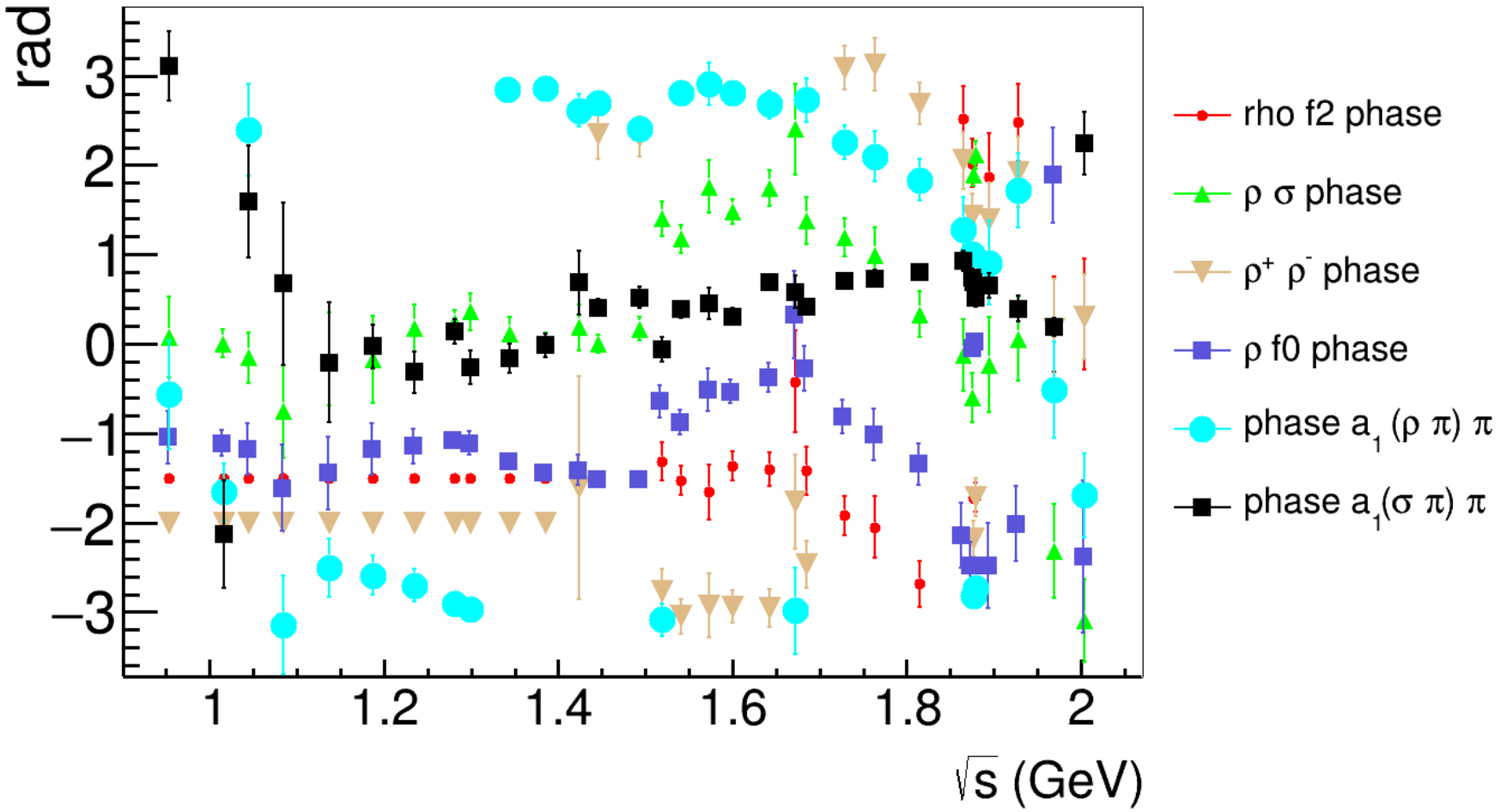

- Neither parameterization of the amplitude does not describe the energy dependence of the phase

$$R_i = \frac{\int |A_i|^2 dPh}{\int |\Sigma_i V_i A_i|^2 dPh} \cdot \sigma_{2\pi^0\pi^+\pi^-}$$

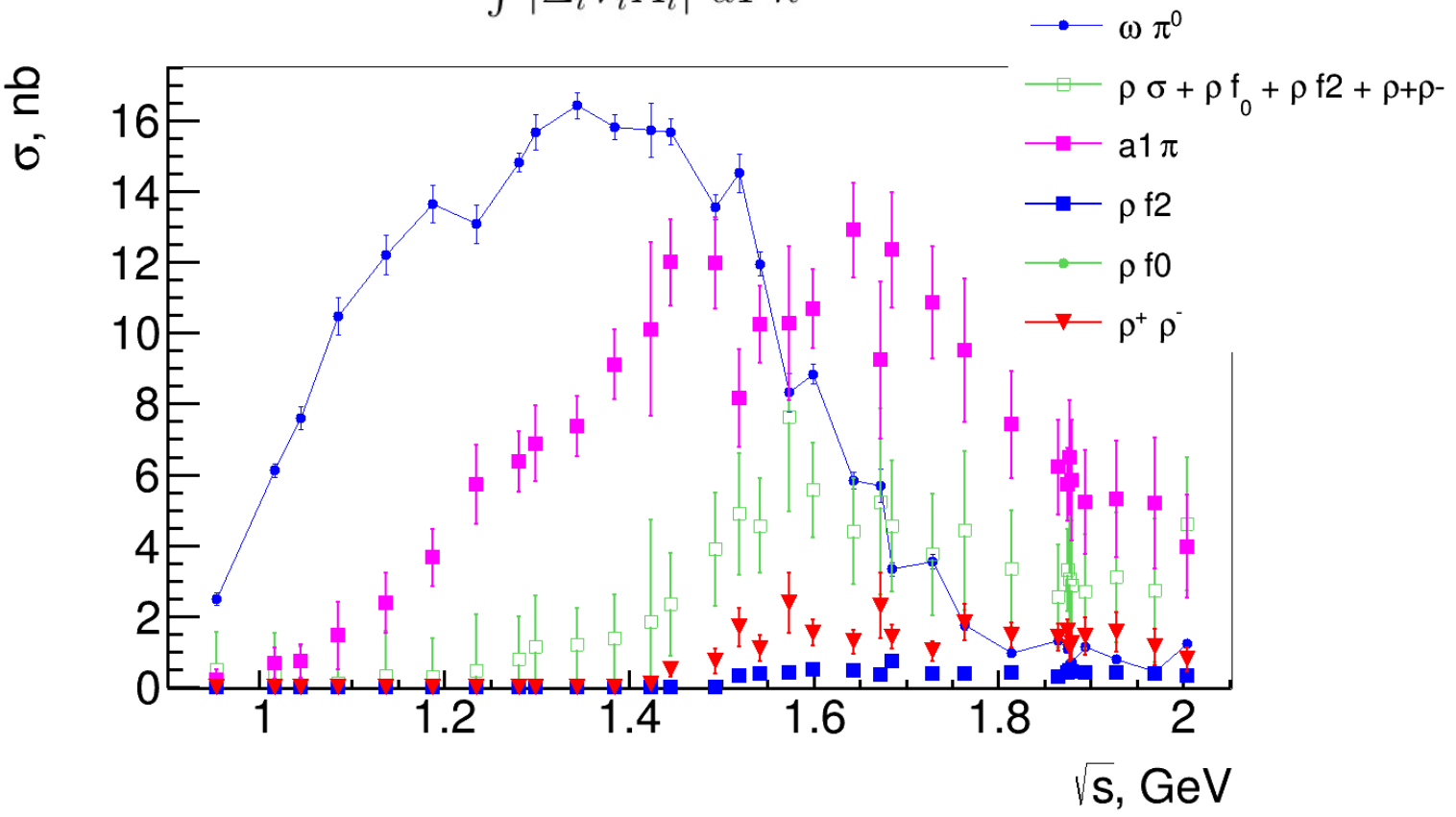

The cross-section of different contribution vs $E_{c.m.}$

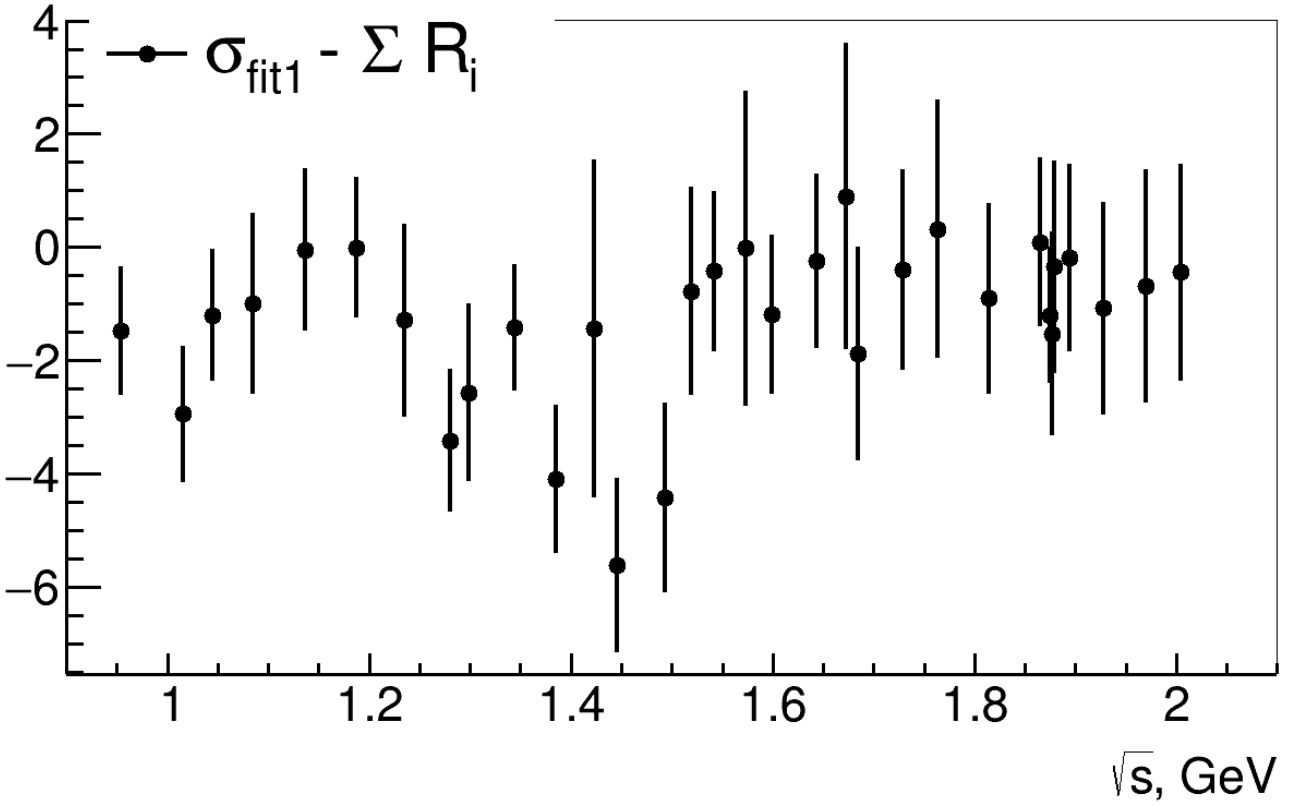

The cross-section of $e^+e^- \to \omega\pi^0 \to \pi^+\pi^-2\pi^0$ with subtracted sum of R_i

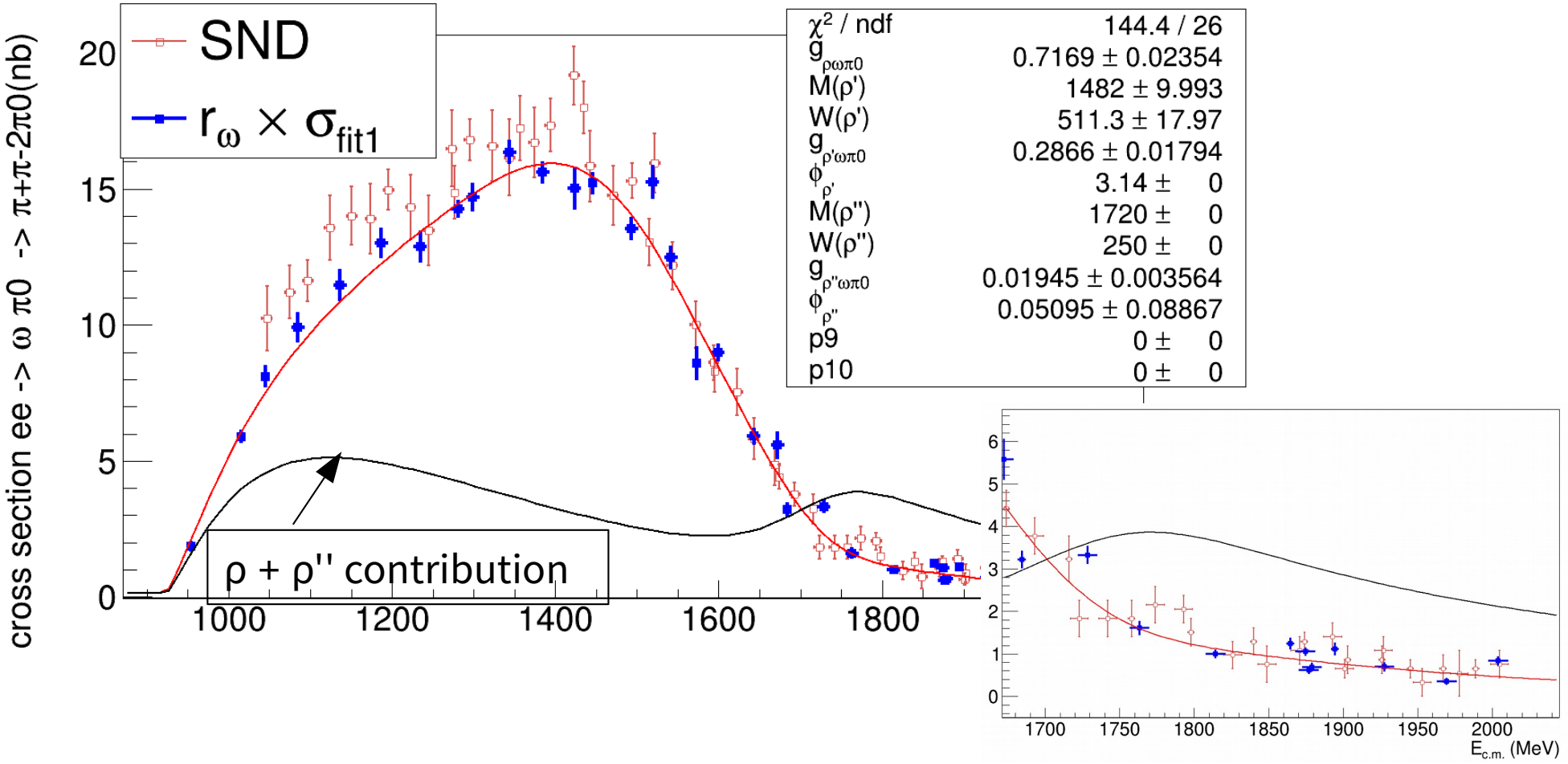

The cross-section of $e^+e^- \to \omega\pi^0 \to \pi^+\pi^-2\pi^0$ vs $E_{c.m.}$

Summary

- The internal dynamics of the reaction $e^+e^-\to4\pi$ is studied preliminary in the energy range $\sqrt{s}$ = [0.95–2.01] GeV

- The dominance of the channels $\omega\pi$ and $a_1\pi$ is confirmed.

- The $\omega\pi$ channel is dominated in the process e+e- → π+π-2π0 up to $\sqrt{s}$ ~ 1.5 GeV

- The estimation of the contributions of $\rho\sigma$, ρf_0, $\rho^-\rho^+$, ρf_2 is shown.

- The simultaneous analysis of $e^+e^-\to2\pi^+2\pi^-$, $e^+e^-\to\pi^+\pi^-2\pi^0$, $\tau^-\to\pi^-3\pi^0\nu$, $\tau^-\to2\pi^-\pi^+\pi^0\nu$ is proposed

back-up

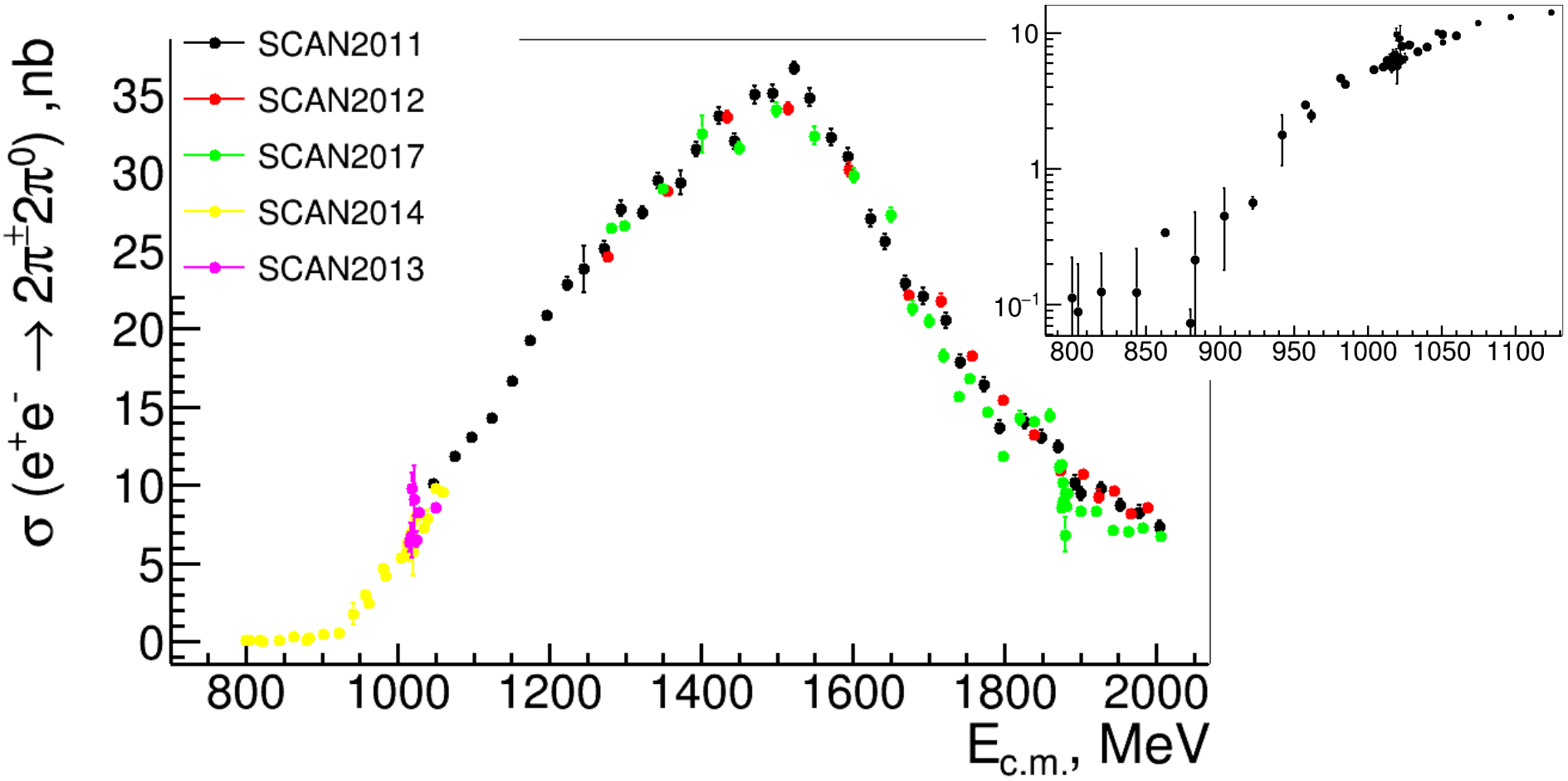

The cross-section of $e^+e^- \to 2\pi^0\pi^+\pi^-$ vs $E_{c.m.}$ for different scans

Soon we will publish the cross section of the cross section

$$\varepsilon_{4\pi} = \frac{\Sigma_{det}^{ph.sp.}(|M(p_{\pi^0},p_{\pi^0},p_{\pi^+},p_{\pi^-})|^2)}{\Sigma_{gen}^{ph.sp.}(|M(p_{\pi^0},p_{\pi^0},p_{\pi^+},p_{\pi^-})|^2)}$$

The max energy of simulated ISR is 0.2 Gev.

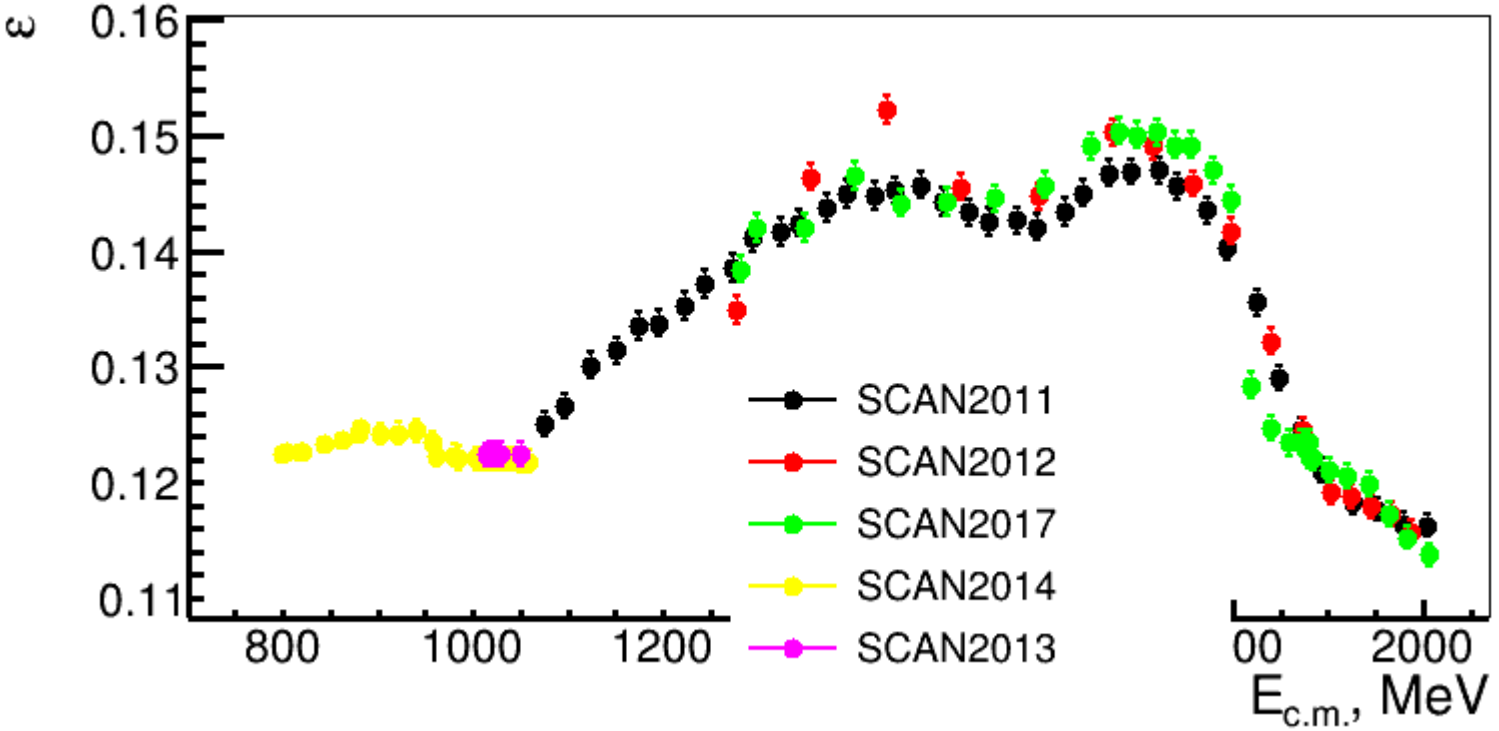

Detection efficiency vs. c.m. energy.

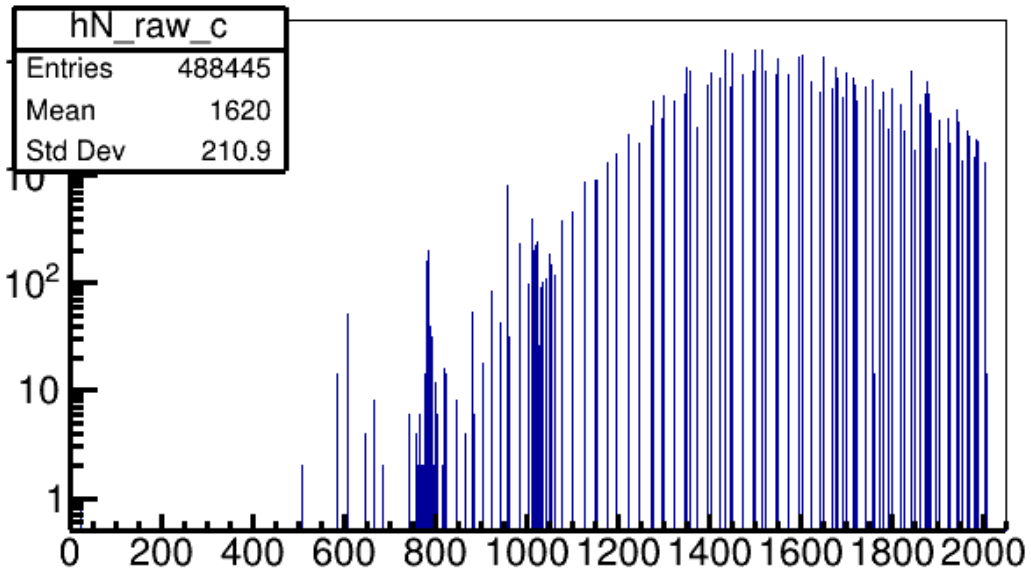
hN_raw_c
Entries 488445
Mean 1620
Std Dev 210.9
10^2
10
1
0 200 400 600 800 1000 1200 1400 1600 1800 2000

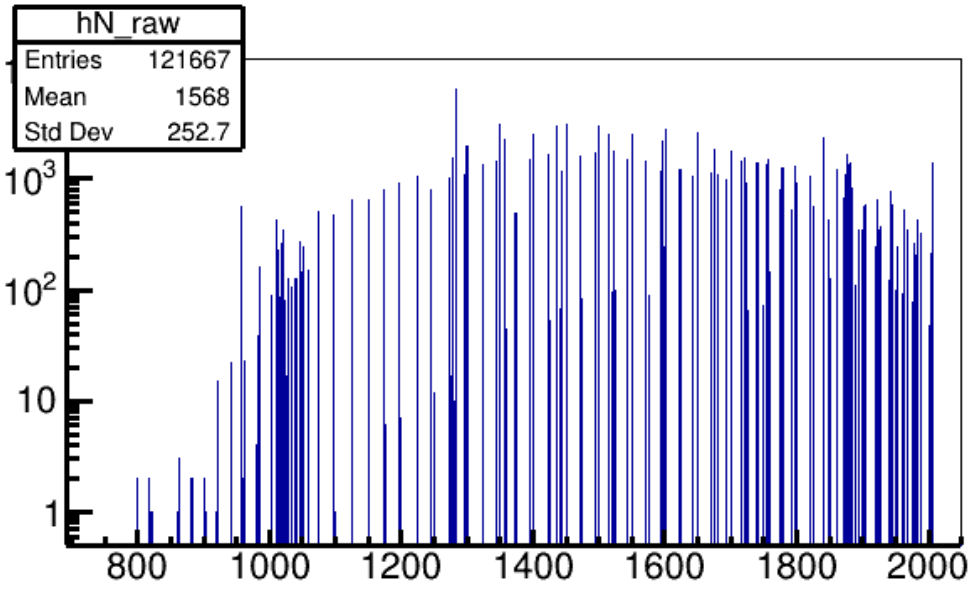
hN_raw
Entries 121667
Mean 1568
Std Dev 252.7
10^3
10^2
10
1
800 1000 1200 1400 1600 1800 2000

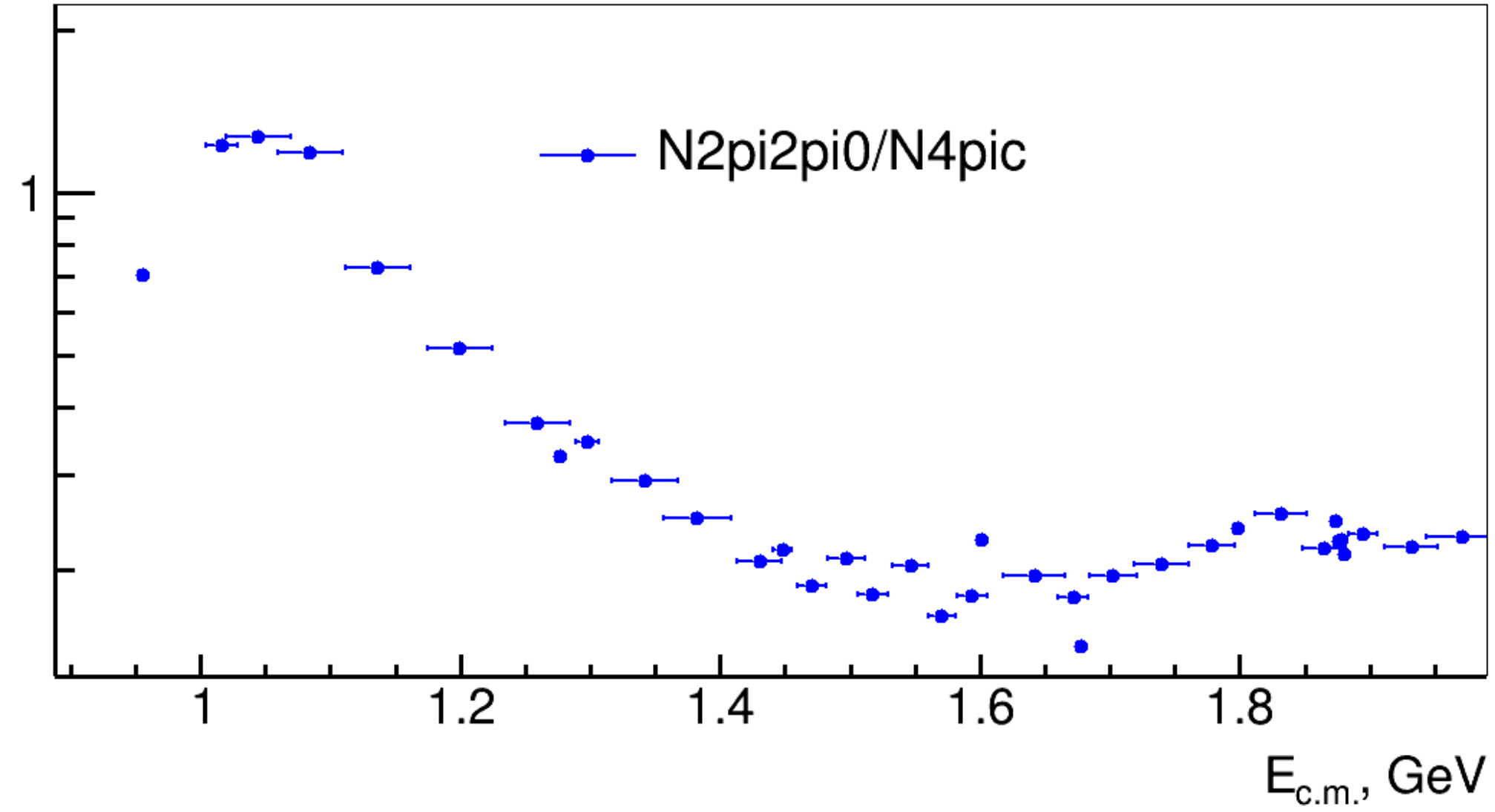
N2pi2pi0/N4pic
1
1
1.2
1.4
1.6
1.8
E_c.m., GeV

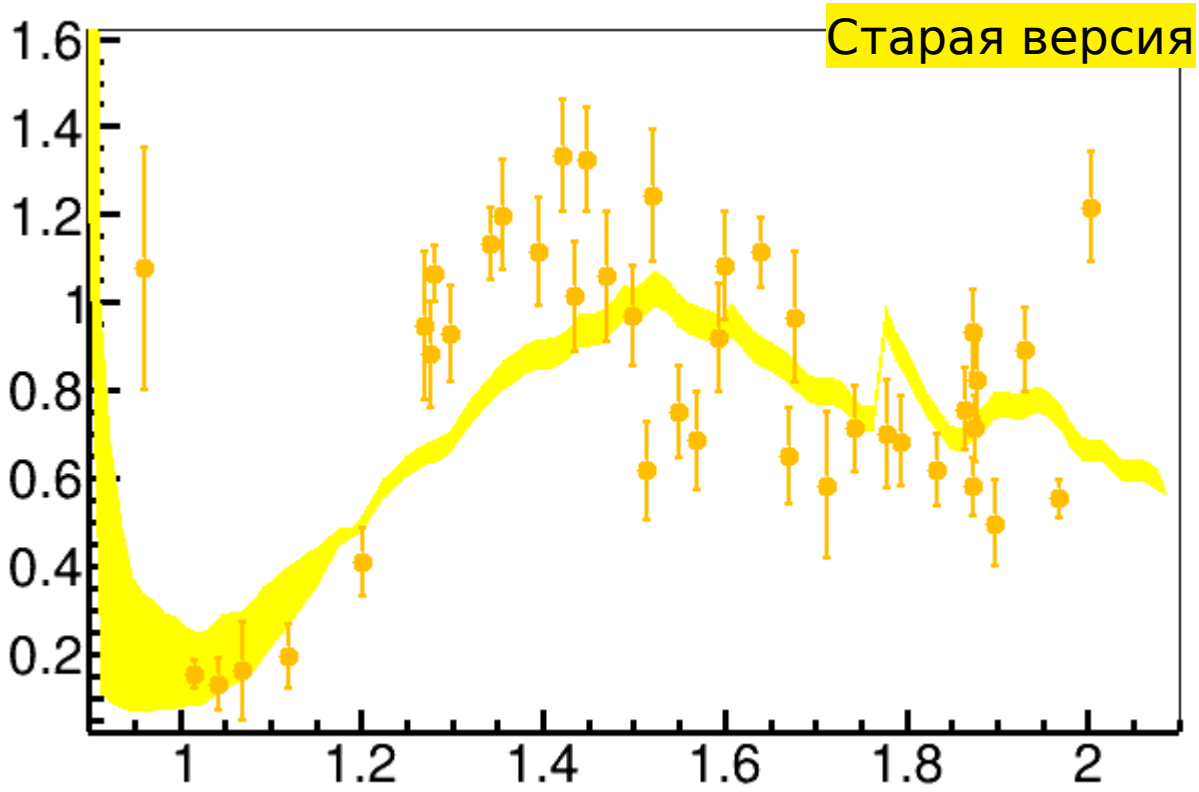

Отношение сечений e+e- \to 2pi+2pi- к e+e- \to pi+pi-2pi0.
Закрашенная область — эксперимент (из др. работ).
Точки с ошибками — результат амплитудного анализа (из данной работы).

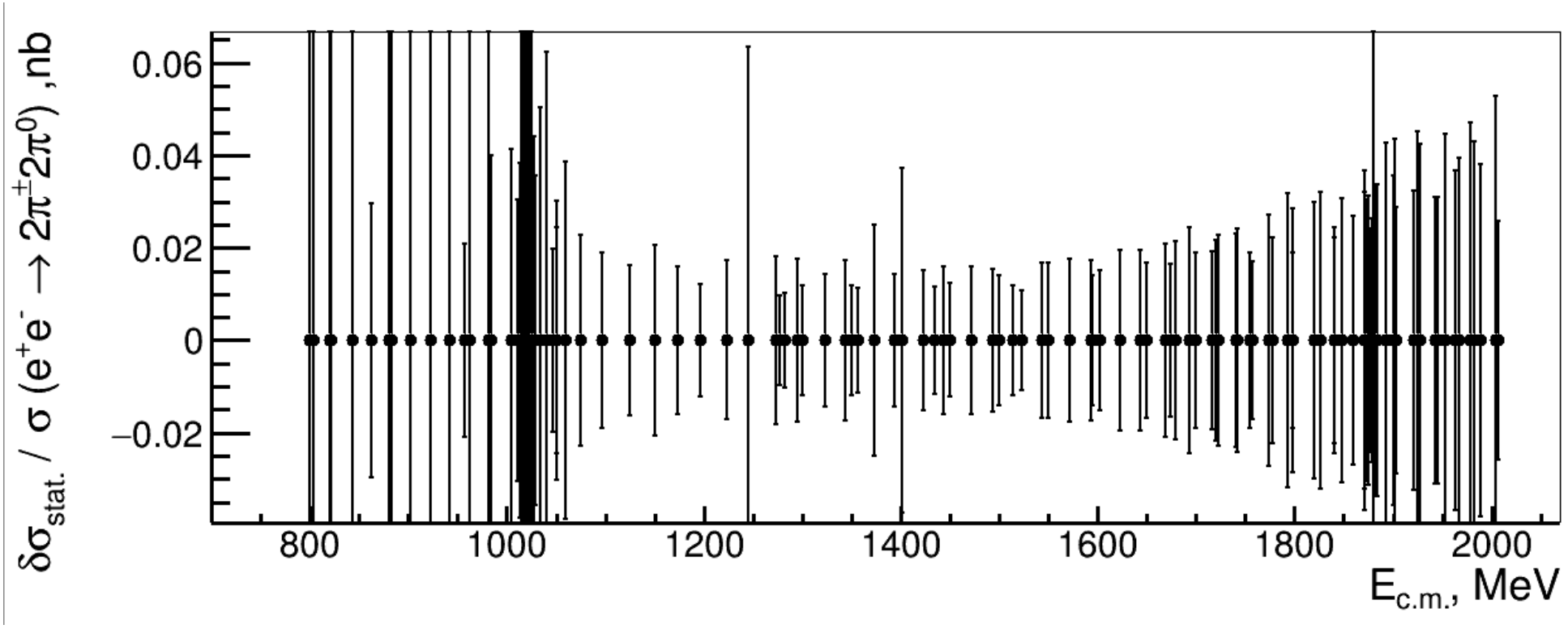

Statistical precision is about 2-3% in average